Stress-Activated Mitogen-Activated Protein Kinases c-Jun NH_2-Terminal Kinase and p38 Target Cdc25B for Degradation

Sanae Uchida,[1,2] Katsuji Yoshioka,[3] Ryoichi Kizu,[4] Hitoshi Nakagama,[5] Tsukasa Matsunaga,[1] Yukihito Ishizaka,[6] Randy Y.C. Poon,[7] and Katsumi Yamashita[1]

[1]Division of Life Science, Graduate School of Natural Science and Technology, [2]Venture Business Laboratory, Center for Innovation, and [3]Division of Molecular Cell Signaling, Cancer Research Institute, Kanazawa University, Kanazawa, Japan; [4]Laboratory of Environmental Biochemistry, Faculty of Pharmaceutical Science, Doshisha Women's College of Liberal Arts, Kyotanabe, Japan; [5]Division of Biochemistry, National Cancer Center Research Institute; [6]Division of Intractable Diseases, Research Institute, International Medical Center of Japan, Tokyo, Japan; and [7]Department of Biochemistry, Hong Kong University of Science and Technology, Clear Water Bay, Hong Kong

Abstract

Cdc25 dual specificity phosphatases positively regulate the cell cycle by activating cyclin-dependent kinase/cyclin complexes. Of the three mammalian Cdc25 isoforms, Cdc25A is phosphorylated by genotoxic stress–activated Chk1 or Chk2, which triggers its $SCF^{\beta\text{-}TrCP}$–mediated degradation. However, the roles of Cdc25B and Cdc25C in cell stress checkpoints remain inconclusive. We herein report that c-Jun NH_2-terminal kinase (JNK) induces the degradation of Cdc25B. Nongenotoxic stress induced by anisomycin caused rapid degradation of Cdc25B as well as Cdc25A. Cdc25B degradation was dependent mainly on JNK and partially on p38 mitogen-activated protein kinase (p38). Accordingly, cotransfection with JNK1, JNK2, or p38 destabilized Cdc25B. *In vitro* kinase assays and site-directed mutagenesis experiments revealed that the critical JNK and p38 phosphorylation site in Cdc25B was Ser^{101}. Cdc25B with Ser^{101} mutated to alanine was refractory to anisomycin-induced degradation, and cells expressing such mutant Cdc25B proteins were able to override the anisomycin-induced G_2 arrest. These results highlight the importance of a novel JNK/p38-Cdc25B axis for a nongenotoxic stress–induced cell cycle checkpoint. [Cancer Res 2009;69(16):6438–44]

Introduction

Cell cycle progression in eukaryotic cells requires the successive activation and inactivation of cyclin-dependent kinase (CDK)-cyclin complexes. Activation of CDK-cyclin complexes depends on members of the Cdc25 dual specificity phosphatases. In mammalian cells, the Cdc25 family consists of Cdc25A, Cdc25B, and Cdc25C. Although Cdc25C was the first member to be identified, Cdc25A is now regarded as one of the major players in multiple phases of cell cycle progression in mammalian somatic cells (1, 2). Besides its well-known role in G_1-S transition, Cdc25A is also involved in the G_2-M transition and chromosome condensation (1, 3, 4). Moreover, Cdc25A is also a well-known target of the DNA damage checkpoint (2, 5). On genotoxic insults, Cdc25A is rapidly phosphorylated by the checkpoint kinases Chk1 and Chk2 followed by $SCF^{\beta\text{-}TrCP}$–mediated ubiquitinylation and degradation (2, 6).

In contrast to Cdc25A, the roles of Cdc25B and Cdc25C remain elusive. Experiments with Cdc25B- or Cdc25C-knockout mice indicate that these genes are dispensable not only for normal cell cycle control but also for the DNA damage checkpoint (7, 8). The only prominent phenotype is a defect in oocyte maturation in Cdc25B-depleted female mice (9). However, several lines of evidence suggest that Cdc25B is important for controlling CDK1-cyclin B activity at the centrosome, where the kinase contributes to centrosome separation at prophase (4, 10). Chk1 is believed to down-regulate the activity of Cdc25B until prophase (11, 12). The phosphorylation of Cdc25B (Ser^{309} of Cdc25B1 or Ser^{323} in Cdc25B3) has also been implicated in the function of Cdc25B in conjunction with 14-3-3 binding (13, 14). A mutation that abolishes the specific phosphorylation site causes Cdc25B to localize to the nucleus and enhances its ability to abrogate DNA damage–induced G_2 arrest (15, 16). These results suggest that despite its nonessentiality in mouse models, Cdc25B does play some role in the G_2-M transition (14).

Stress stimuli that do not target genome DNA lead to the activation of the so-called stress-activated mitogen-activated protein kinases (MAPK), including p38 MAPK (p38) and c-Jun NH_2-terminal kinase (JNK; ref. 17). Recently, MAPKAP kinase 2 (MK2) has received attention for its ability to phosphorylate Cdc25B, leading to 14-3-3 binding (18). MK2 is usually complexed with and activated by p38 (18). Therefore, a fraction of p38 can be found to coimmunoprecipitate with MK2, which could mislead one to believe that p38 phosphorylates substrates that are normally phosphorylated exclusively by MK2. The p38-MK2 cascade is, therefore, believed to regulate cell cycle progression by controlling the stability and subcellular localization of Cdc25A and Cdc25B, respectively, when cells are exposed to genotoxic or nongenotoxic stress (14, 18–20). JNK also phosphorylates and inactivates Cdc25C (21). In addition, nuclear Cdc25B is exported to the cytoplasm on UV or nongenotoxic stress by an unknown mechanism (22).

We previously reported that overexpression of 14-3-3 causes the relocation of Cdc25B from the nucleus to the cytoplasm (13, 23, 24). To delineate the role of the cytoplasmic export of Cdc25B, we established HeLa cell lines that constitutively express Cdc25B and investigated conditions that induce nuclear export of the phosphatase. We found that nongenotoxic stress, but not genotoxic cell stress, induced loss of Cdc25B nuclear localization and that nongenotoxic stress was also an effective inducer of Cdc25B degradation. Moreover, we found that the stability of Cdc25B could be controlled by JNK and p38. These data reveal a novel pathway linking the stress response kinases to the G_2-M cell cycle engine.

Materials and Methods

Reagents, plasmids, and antibodies. Reagents of the highest grade were obtained from Wako or Sigma. Restriction enzymes were obtained from New England Biolabs, and MKK7-activated recombinant JNK1 and

Note: Supplementary data for this article are available at Cancer Research Online (http://cancerres.aacrjournals.org/).

Requests for reprints: Katsumi Yamashita, Division of Life Sciences, Graduate School of Natural Science and Technology, Kanazawa University, Kakuma-machi, Kanazawa 920-1192, Ishikawa, Japan. Phone: 81-76-264-6270; Fax: 81-76-264-6270; E-mail: katsumi@kenroku.kanazawa-u.ac.jp.

doi:10.1158/0008-5472.CAN-09-0869

MKK6-activated p38α (both isolated from baculovirus-infected Sf21 cells) were obtained from Upstate. Oligonucleotides were synthesized by Invitrogen. The cDNAs and antibodies used in the experiments were described in Supplementary Materials and Methods.

Cell culture and plasmid transfection. HeLa cells were grown in DMEM as previously described (13). Plasmids were transiently transfected with Lipofectamine 2000 (Invitrogen). Cell cycle synchronization was performed using the double thymidine block protocol. To obtain stable Flag-tagged Cdc25B (F-Cdc25B)–expressing HeLa cells, we used 10 μg/mL blasticidin S (Invitrogen) for the selection of transformed cells. Established Flag-Cdc25B–expressing HeLa cells were maintained with 2 μg/mL blasticidin S.

Preparation of crude extracts, immunoblotting, immunoprecipitation, and kinase assay. Crude extracts for the analysis of proteins followed by immunoblotting or immunoprecipitation were performed as described previously (13). To detect endogenous Cdc25B, we subjected proteins that had been immunoprecipitated with rabbit anti-Cdc25B antibodies to SDS-PAGE, followed by immunoblotting. The Cdc25B protein was detected with mouse monoclonal anti-Cdc25B antibody. The immunoprecipitates used for the kinase assay were washed twice with buffer containing 100 mmol/L Tris-HCl (pH 8.0), 5 mmol/L EGTA, and 20 mmol/L $MgCl_2$. The samples were then incubated with the same buffer that was supplemented with appropriate glutathione *S*-transferase (GST) fusion Cdc25B proteins, 1 mmol/L DTT, 200 μmol/L ATP, and [γ-^{32}P]ATP (1 μCi = 37 KBq; Perkin-Elmer). The reaction mixtures were incubated at 30°C for 60 min and subjected to SDS-PAGE, and radioactivity was detected using the Fuji BAS system (Fujifilm).

Indirect immunofluorescence and flow cytometry. Indirect immunofluorescence of cells grown on glass coverslips was conducted as described previously (13). Cells treated for fluorescence-activated cell sorting (FACS) were analyzed on a FACSCalibur (BD Biosciences) using ModFit software. The Ser^{10}-phosphorylated histone H3 (phospho-S10-H3)–positive cells were analyzed using CellQuest software.

Results

Nuclear localization of Cdc25B is lost following treatment of cells with anisomycin but not with DNA-damaging agents. Phosphorylation of Ser^{309} of Cdc25B1 followed by binding of 14-3-3 disrupts nuclear localization of Cdc25B (13). Ser^{309} can be phosphorylated by Chk1/2 and MK2 (18, 25, 26). To determine the types of cellular stresses that induce nuclear export, we treated cells with various chemicals and analyzed the subcellular localization of Cdc25B. Given that an antibody that displayed high specificity toward endogenous Cdc25B was not available commercially or in house, we first established a HeLa cell–based cell line that constitutively expressed F-Cdc25B. No gross abnormality of cell growth or morphology was discerned for F-Cdc25B–expressing cells, which are hereafter called HeLa-W40 cells.

We treated HeLa-W40 cells with hydroxyurea, aphidicolin, etoposide, or camptothecin, which activate either Chk1 or Chk2. DNA damage induced by the chemicals was confirmed by assaying for phosphorylated histone H2AX (γ-H2AX; ref. 27). Cdc25B localized to the nucleus in cells with or without DNA damage or replication arrest (Fig. 1*A*). We next investigated the possible involvement of the p38/MK2 pathways in this process. To activate the p38/MK2 pathway, we treated the cells with anisomycin, which activates p38 and JNK (28, 29). Treatment with anisomycin disrupted the nuclear localization of Cdc25B and promoted the redistribution of Cdc25B to the cytoplasm (Fig. 1*B*). These results suggest that Cdc25B nuclear localization can be disrupted by stress pathways other than those initiated by DNA damage.

To assess the possibility that the p38 pathway regulates Cdc25B, we added the p38 inhibitor SB202190 to HeLa-W40 cells. Of interest

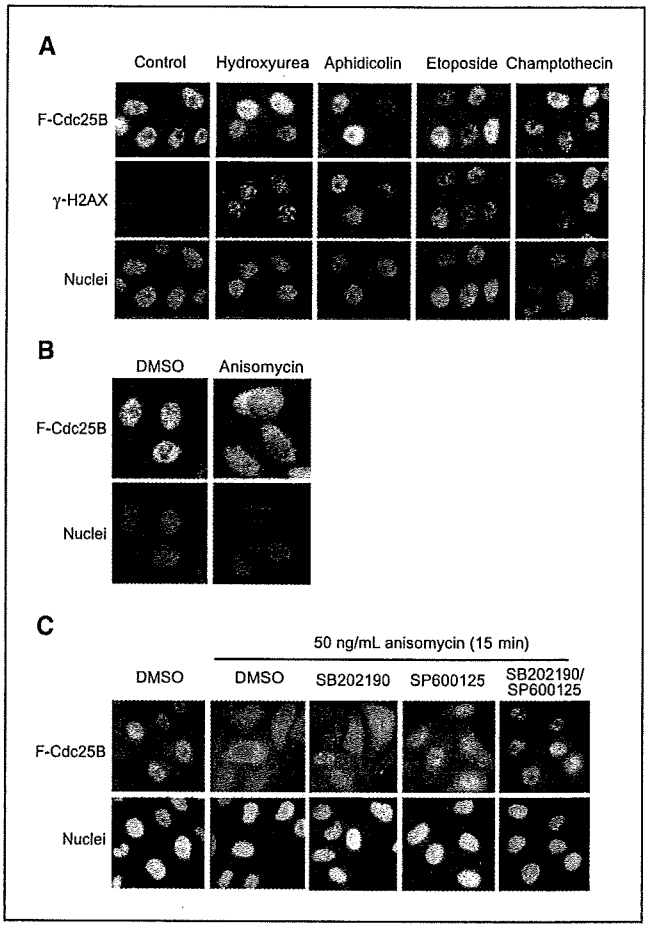

Figure 1. Nuclear localization of Cdc25B is maintained after DNA damage but is disturbed by anisomycin treatment. *A*, HeLa-W40 cells were treated with the indicated chemicals and Flag-Cdc25B and γ-H2AX were detected by indirect immunofluorescence. The nuclei were identified using 4′,6-diamidino-2-phenylindole. The conditions for chemical treatment were described in Supplementary Materials and Methods. *B*, HeLa-W40 cells were treated with 50 ng/mL anisomycin for 15 min and processed for indirect immunofluorescence. *C*, HeLa-W40 cells were pretreated with the indicated MAPK inhibitors for 1 h followed by anisomycin challenge. The cells were fixed, and Flag-Cdc25B and nuclei were analyzed. The concentration for inhibitors was as follows: SB202190, 20 μmol/L; SP600125, 20 μmol/L.

is that SB202190 exerted only a small effect on the anisomycin-induced diffusion of Cdc25B (Fig. 1*C*). In contrast, the JNK inhibitor SP600125 induced strong nuclear staining of Cdc25B under conditions of anisomycin stress. Furthermore, stronger nuclear signals for Cdc25B were generated by simultaneous treatment with both SB202190 and SP600125 than by treatment with SP600125 alone. Inhibition of MAPK/extracellular signal-regulated kinase (ERK) kinase (MEK1) with U0126, thereby inhibiting the activation of ERK1/2, did not prevent cytoplasmic diffusion of Cdc25B (data not shown). Collectively, these data indicate that anisomycin-mediated stress can disrupt nuclear localization of Cdc25B in a JNK-dependent manner.

Cdc25B is degraded in cells treated with anisomycin or sodium chloride but not with DNA-damaging agents. The signals for F-Cdc25B faded in cells after long-term exposure to anisomycin but not after treatment with DNA-damaging agents (data not shown). These observations led us to analyze the level of F-Cdc25B protein in HeLa-W40 cells treated with anisomycin and another

nongenotoxic reagent, sodium chloride (NaCl). We also examined the levels of Cdc25A and Cdc25C to determine whether different cellular stresses affect members of this phosphatase family. Genotoxic stress caused by exposure to hydroxyurea, aphidicolin, etoposide, or camptothecin effectively induced Cdc25A degradation (Fig. 2*A*). In contrast, expression of Cdc25B or Cdc25C was unaffected under the same conditions. Although neither anisomycin nor NaCl activated Chk1 or Chk2, both Cdc25B and Cdc25A were degraded (Fig. 2*A*). Cdc25A and Cdc25B decreased in a time-dependent fashion after exposure to anisomycin (Fig. 2*B*). The endogenous Cdc25B protein in parental HeLa cells was also degraded by anisomycin treatment but not by DNA-damaging agents (Supplementary Fig. S1). The abundance of Cdc25C was not affected by any of the stimuli examined here. UV irradiation, which is known to activate not only Chk1/2 but also p38/JNK, abrogated nuclear localization of Cdc25B as reported (22) and induced Cdc25B degradation (Supplementary Fig. S2*A* and *B*).

Although anisomycin inhibits protein synthesis (29), the more rapid decline of Cdc25B in anisomycin-treated cells compared with cycloheximide-treated cells suggested that degradation of Cdc25B was specifically caused by anisomycin-induced stress and not by a general inhibition of protein synthesis (Fig. 2*C*). More convincing evidence was obtained when we examined the stability of Cdc25B that contained mutations at the constitutive β-TrCP binding site of ^{254}DDGFVD^{259} (amino acid numbering is based on human Cdc25B1; ref. 30). The site is responsible for the steady-state degradation of Cdc25B by a constitutive SCF$^{\beta\text{-TrCP}}$–mediated ubiquitin-proteasome pathway. We established a HeLa cell line expressing a mutant Cdc25B that contained mutations at the β-TrCP binding site (Cdc25B^{DAA}, of which D255 and G256 were replaced by Ala). Figure 2*D* shows that Cdc25B^{DAA} was unstable after anisomycin treatment. This indicates that the Cdc25B degradation was specific to anisomycin treatment. Collectively, these data indicate that anisomycin-induced stress, but not DNA damage-induced stress, triggers a loss of nuclear localization and stability of Cdc25B.

Inhibition of JNK attenuates the degradation of Cdc25B by anisomycin. To determine the role of p38 or JNK on the stability of Cdc25A and Cdc25B, we treated HeLa cells with inhibitors of p38 or JNK and analyzed the cellular proteins. The activation of p38α/β was monitored as the slower migrating form of MK2, corresponding to phosphorylated MK2 (Fig. 3*A*); JNK activation was monitored using antibodies recognizing phospho-JNK1 or phospho–c-Jun. We found that the JNK inhibitor SP600125 protected Cdc25B from anisomycin-induced degradation (Fig. 3*A*, *lanes 5-8*). A relatively small but definite contribution of the p38 pathway to the degradation of Cdc25B was revealed by these experiments (Fig. 3*A*, *lanes 3–8*). The MEK1 inhibitor U0126 again had no effect on the stability of either Cdc25A or Cdc25B (data not shown). Time course experiments further validated the critical role of JNK in regulating the degradation of Cdc25B (Fig. 3*B*). The stability of Cdc25C was essentially unaffected by these inhibitors (Fig. 3*A*). Exactly the same results were obtained with HeLa-W40 cells that expressed F-Cdc25B (Supplementary Fig. S3*A*). JNK inhibitor also attenuated the NaCl-induced F-Cdc25B degradation (Supplementary Fig. S3*B*). Results shown in Fig. 3*C* indicate the correlation between the degradation of Cdc25A/Cdc25B and activation of p38/JNK. Anisomycin-, NaCl-, or UV-induced degradation of Cdc25B was inhibited by the proteasome inhibitor MG132, suggesting that the anisomycin-induced degradation of Cdc25B is mediated by the ubiquitin-proteasome pathway (Supplementary Fig. S3*C*, *1*, *2*, and *3*).

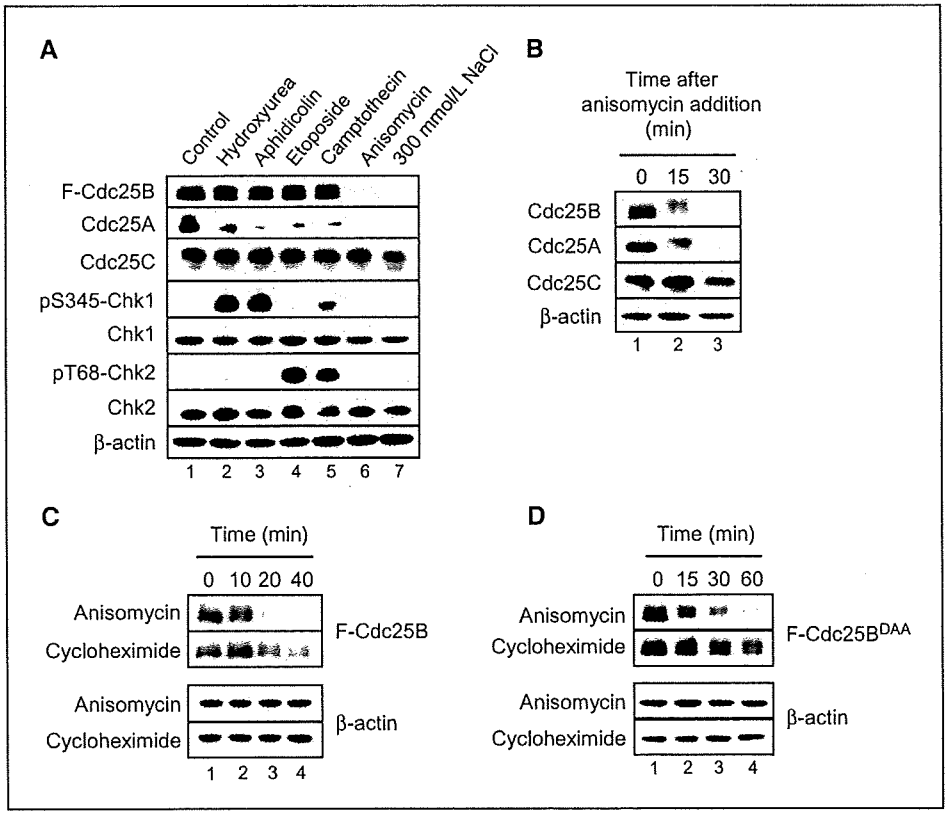

Figure 2. Degradation of Cdc25A and Cdc25B after treatment with DNA-damaging or non–DNA-damaging agents. *A*, HeLa-W40 cells were treated with genotoxic chemicals as described in Supplementary Materials and Methods. The cells were incubated with anisomycin or 300 mmol/L NaCl for 30 min or 1 h, respectively. Cell extracts were prepared, and indicated proteins were detected by immunoblotting. β-Actin analysis serves as a loading control. *B*, parental HeLa cells were treated with anisomycin, and cell extracts were prepared at the indicated time to detect endogenous Cdc25A, Cdc25B, and Cdc25C. *C*, HeLa-W40 cells were treated with anisomycin or 50 μg/mL cycloheximide. Crude extracts were prepared at the indicated time, and the expression of Flag-Cdc25B was analyzed. *D*, HeLa cells constitutively expressing the Cdc25B^{DAA} mutant were treated with anisomycin or cycloheximide and the expression of Flag-Cdc25B proteins was determined by immunoblotting.

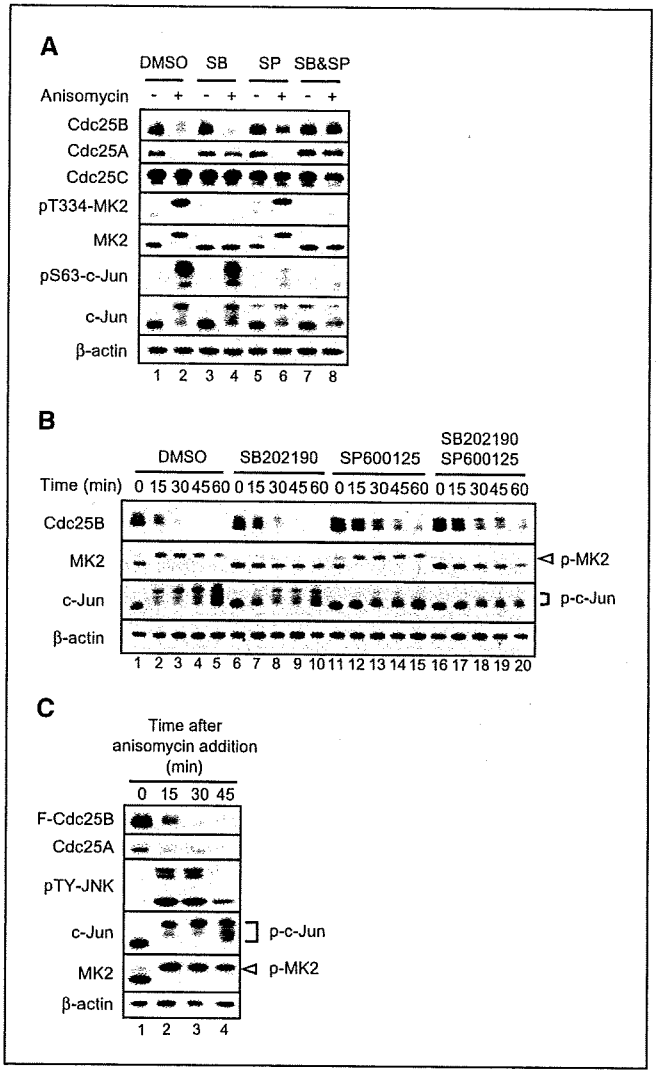

Figure 3. JNK inhibitor SP600125 attenuates the anisomycin-induced Cdc25B degradation. *A*, HeLa cells were treated with the indicated MAPK inhibitors for 1 h followed by anisomycin treatment. Cell extracts were prepared at 20 min after anisomycin addition. *SB*, SB202190; *SP*, SP600125. *B*, HeLa cells were treated with MAPK inhibitors, and the expression of proteins was determined at the indicated time. *C*, HeLa-W40 cells were treated with anisomycin, and the expression of protein was determined at the indicated time. Slower migrating bands of c-Jun and MK2 represent phosphorylated forms of the proteins.

Results of indirect immunofluorescence also supported that the instability of Cdc25B in anisomycin-treated cells was due to its proteasome-dependent degradation (Supplementary Fig. S3*D*).

The coexpression of either JNK1 or JNK2 with MKK7 triggered Cdc25B degradation (Fig. 4*A*). In addition, p38α was able to induce Cdc25B degradation. Furthermore, the expression of kinase-dead JNK1 and JNK2 stabilized Cdc25B (Fig. 4*B*), indicating dominant-negative effects. We further examined the contribution of MK2 to Cdc25B degradation. In this experiment, we used the D316N mutant of p38α, which is unable to activate MK2 (31). As shown in Fig. 4*C*, expression of $p38\alpha^{D316N}$ induced the degradation of Cdc25B. Taken together, these results suggest that JNK and p38 are integrally involved in Cdc25B degradation.

JNK phosphorylates Cdc25B. We found that bacterially expressed Cdc25B was phosphorylated by kinase-active JNK1 but not by its kinase-dead form, indication that JNK1 can directly phosphorylate Cdc25B (Supplementary Fig. S4*A*). Likewise, recombinant JNK1 could also phosphorylate Cdc25B (Supplementary Fig. S4*B*). To identify the phosphorylation site(s) on Cdc25B, GST fusion constructs of different fragments of Cdc25B were produced in *Escherichia coli* and used as substrates for kinase assays. As shown in Fig. 5*A*, JNK phosphorylation sites were present in the NH_2-terminal 175 amino acids. The same fragment was also phosphorylated by recombinant p38α (Supplementary Fig. S4*C*). Furthermore, JNK and Cdc25B were able to form complex, which supports the idea of Cdc25B being a JNK substrate [Supplementary Fig. S5*A*; the loss of the complex formation in wild-type (WT) JNK with MKK7 suggests that JNK may dislodge after phosphorylation event]. The importance of the NH_2-terminal region was also supported by the JNK-induced degradation of the construct containing green fluorescent protein fused to the NH_2-terminal 175 amino acid fragment of Cdc25B (Supplementary Fig. S5*B*).

Cdc25B/S101 is a candidate JNK phosphorylation site. To identify JNK phosphorylation site(s), we first mutated all six candidate serine residues to alanine in six potential JNK substrate SP sequences (and no TP) in N175-Cdc25B. The 6SA mutant was refractory to JNK- or p38α-induced degradation (Supplementary Fig. S6*A*). The coexpression of the individual SA mutant Cdc25B with JNK indicated the importance of S101, followed by S103 (Fig. 5*B*). The importance of S101 and S103 was further supported

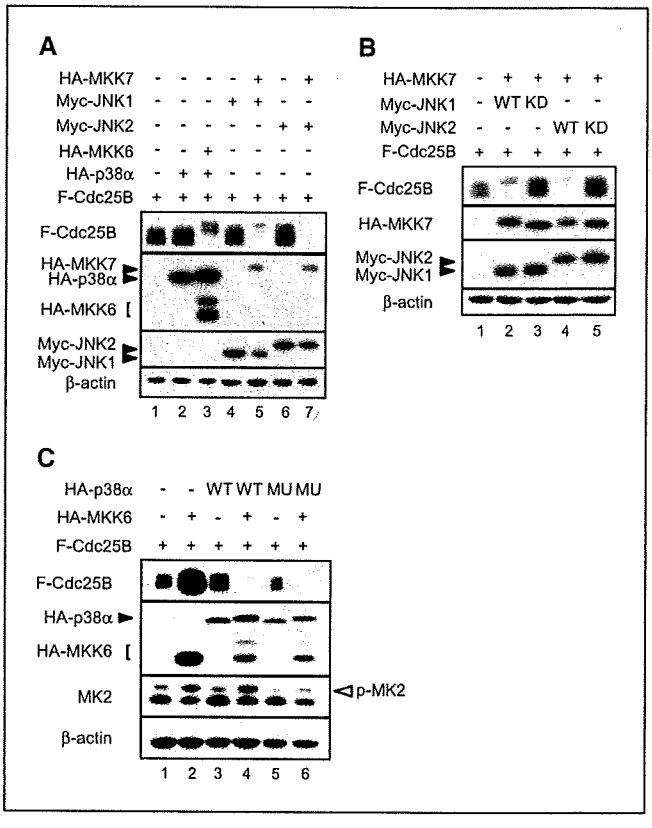

Figure 4. Involvement of JNK in the destabilization of Cdc25B. *A*, HeLa cells were transfected with Flag-Cdc25B in combination with MKK6 and p38α, or MKK7 and JNK1 or JNK2. The expression of the indicated proteins was determined by immunoblotting. *B*, expression of Flag-Cdc25B was determined after cotransfection with MKK7 and either the WT or kinase-dead (*KD*) form of JNK1 or JNK2. *C*, expression of Flag-Cdc25B was examined after cotransfection with MKK6 and WT or the D316N mutant (*MU*) of p38α. *Arrowhead*, phospho-MK2.

by the slower degradation rate of the Cdc25B protein with a double mutation (S101/103A) compared with the mutants with a single mutation (Fig. 5*C, lanes 4, 6,* and *8*). Essentially the same results were obtained when p38α was used as a kinase for the Cdc25B mutants (Supplementary Fig. S6*B*). Taken together, these data indicate that phosphorylation of Cdc25B at S101 and S103 by JNK and p38 is important for degradation.

HeLa cells expressing the Cdc25B S101A mutant ignore anisomycin-induced G_2 arrest. We next examined the effects of anisomycin on cell cycle progression, in particular during G_2-M phase, when Cdc25B peaks during the cell cycle. HeLa cells were synchronized at G_1-S and released into S phase. At 6 hours after release, the cells were treated with anisomycin followed by monitoring of M-phase entry by detection of phospho-S10-H3. Cdc25B and phospho-S10-H3 increased progressively in DMSO-treated cells (Fig. 6*A*), but no phospho-S10-H3 was detected in anisomycin-treated cells, indicating that anisomycin treatment inhibited mitotic entry. In such cells, Cdc25B disappeared completely by 30 minutes after addition of anisomycin (Fig. 6*A, lanes 7* and *8*). FACS analysis confirmed the induction of a G_2 delay by anisomycin treatment in synchronously or asynchronously growing HeLa cells (Supplementary Fig. S7*A*).

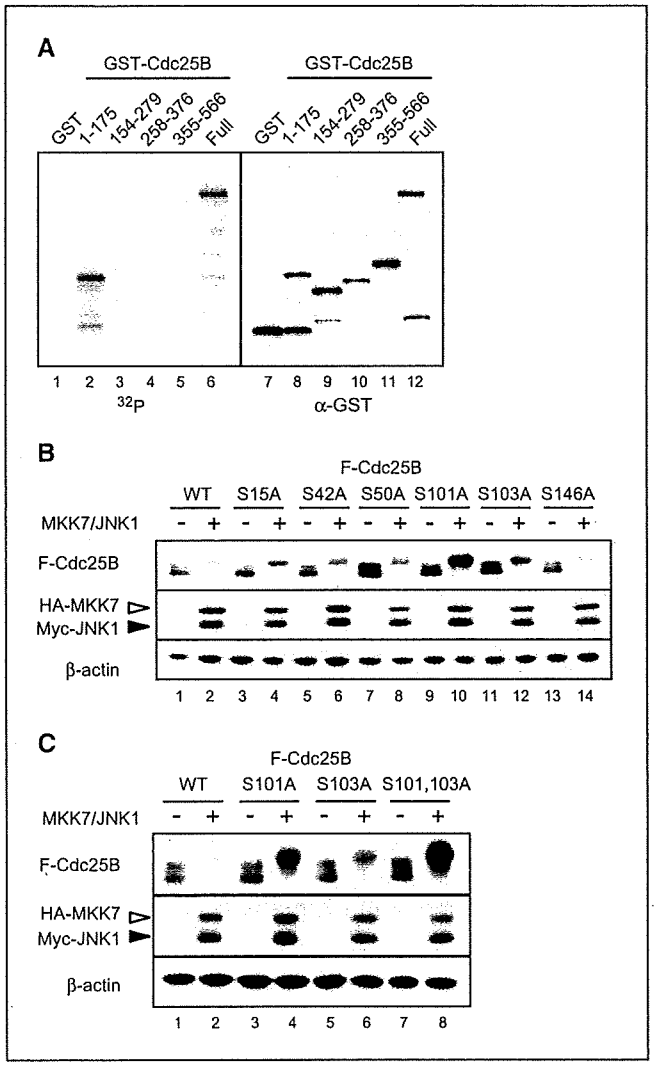

Figure 5. Phosphorylation of Cdc25B by JNK at possible phosphorylation sites. *A, left,* GST-Cdc25B fragments were incubated with a recombinant JNK1 in the presence of [γ-^{32}P]ATP followed by autoradiography; *right,* substrate GST-Cdc25B fragment as detected by anti-GST antibody. *B,* WT Cdc25B or mutants that contained SA mutations at candidate JNK phosphorylation sites were cotransfected into HeLa cells with or without MKK7 and JNK1, and expression of Cdc25B was determined by immunoblotting. *C,* the WT or SA mutant at S101, S103, or S101/103 was cotransfected into HeLa cells with or without MKK7 and JNK1, and the expression of Cdc25B was determined.

To delineate the significance of Cdc25B S101 phosphorylation in anisomycin-induced G_2 arrest, we added anisomycin to asynchronously growing HeLa cells that constitutively express the nonphosphorylatable Cdc25B S101A mutant (HeLa-101-1). The results shown in Fig. 6*B* indicate that the half-life of the S101A mutant Cdc25B was twice as long as that of the WT after anisomycin treatment (~35 minutes in S101A and ~15 minutes in WT), indicating that phosphorylation of S101 is essential for proper degradation. Treatment of HeLa-101-1 with either NaCl or UV also supported the idea that S101 is important for stress-induced Cdc25B degradation (Supplementary Fig. S8*A*).

We next investigated whether the S101A mutant would exhibit abrogation of anisomycin-induced G_2 arrest. We used cell lines expressing WT Cdc25B (W40) or S101A (101-1). The amount of Cdc25B protein in W40 cells and that of 101-1 is shown in Supplementary Fig. S7*B*. Asynchronously growing HeLa cells, W40 cells, and 101-1 cells were treated with 100 ng/mL anisomycin, and the number of cells entering M phase during a 3-hour treatment with anisomycin was determined by detecting phospho-S10-H3. As shown in Fig. 6*C*, HeLa-101-1 cells exhibited resistance to anisomycin-induced G_2 retardation. Thus, cells expressing S101A-mutated Cdc25B seem to be more resistant to anisomycin-induced degradation and to recover more rapidly than WT Cdc25B-expressing cells.

Collectively, HeLa cells expressing Cdc25B with a nonphosphorylatable mutation at the possible JNK target S101 residue were more refractory to anisomycin-induced cell cycle retardation.

Discussion

We report here for the first time that Cdc25B is targeted for degradation in cells that are challenged with anisomycin or NaCl and that the degradation of Cdc25B is mediated mainly by JNK. We uncovered this phenomenon by using HeLa cells that constitutively expressed recombinant Cdc25B. In our hands, commercially available antibodies did not properly recognize endogenous Cdc25B in crude extracts by immunoblotting. Immunoprecipitation followed by immunoblotting was necessary to detect endogenous Cdc25B.

Our experiments highlight the critical role of JNK in controlling Cdc25B stability. A level of DNA damage that is sufficient for activating Chk1/2 and Cdc25A degradation did not exert any effects on the stability of Cdc25B. Export of Cdc25B from the nucleus to the cytoplasm is thought to be a mechanism of checkpoint response (18). However, Cdc25B did not follow this expected pattern after DNA damage (Fig. 1*A*). We therefore suspect that Cdc25B is not a primary target of the DNA damage checkpoint, although we cannot exclude the possibility that its phosphatase activity is directly repressed by a Chk1-dependent mechanism (32).

We showed that M-phase entry is delayed in HeLa cells treated with anisomycin (Fig. 6). The G_2 retardation observed in this situation is caused in part by the degradation of Cdc25A and Cdc25B. Depletion of either Cdc25A or Cdc25B is insufficient for G_2-phase arrest, but the depletion of both Cdc25A and Cdc25B is necessary for a more robust G_2 arrest (4). Therefore, anisomycin-induced G_2

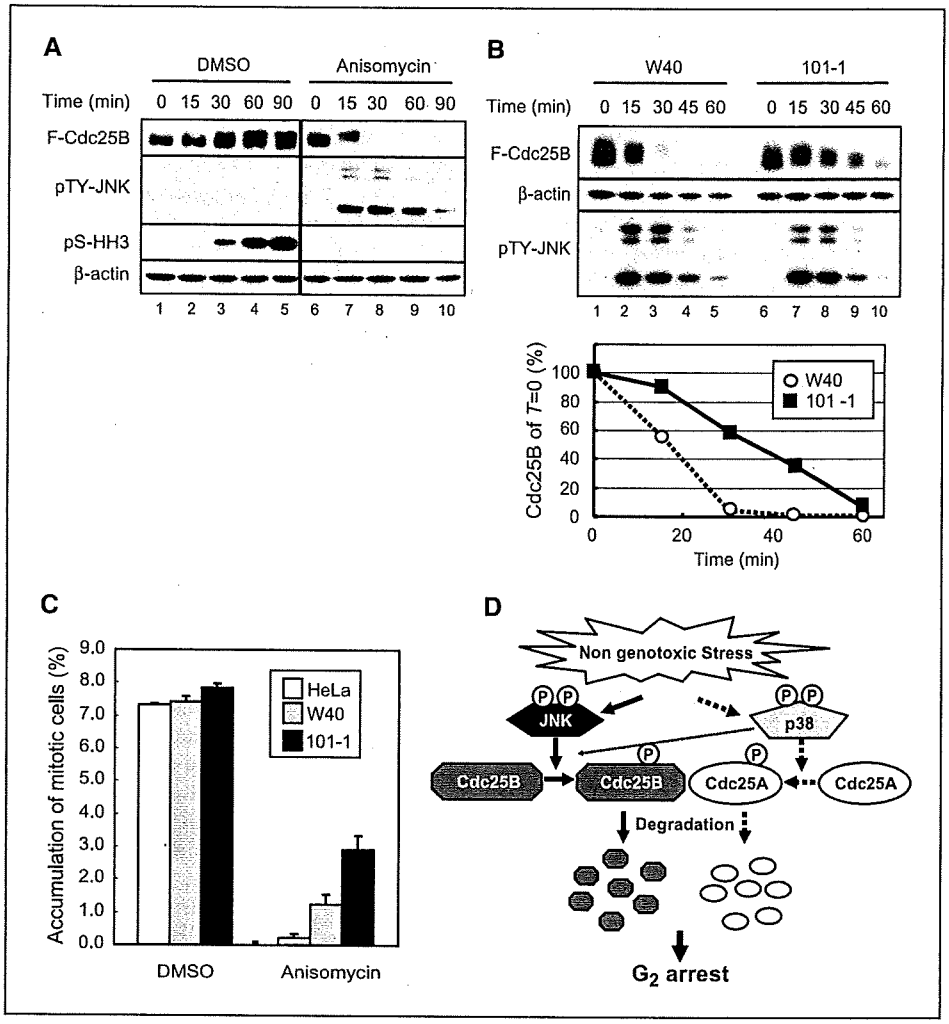

Figure 6. The Cdc25B mutant is refractory to anisomycin-induced G_2 arrest. *A*, HeLa cells synchronized at G_1-S were released into the cell cycle for 6 h, followed by the addition of anisomycin. At the indicated times, the expression of proteins was determined. *B*, HeLa-W40 or HeLa-101-1 cells were treated with anisomycin, and the expression of the proteins was determined at the indicated time points after treatment. *Bottom*, quantitative results. Typical results of three independent experiments are shown. *C*, asynchronously growing HeLa, HeLa-W40, or HeLa-101-1 cells were treated with 100 ng/mL anisomycin and 100 ng/mL nocodazole for 3 h. Cells were collected, and the cells in M phase were determined by detecting phospho-histone H3-Ser[10] by FACS. *Columns*, mean of three independent experiments; *bars*, SD. The percentage of mitotic cells in asynchronous cells was as follows: HeLa, 2.76 ± 0.27; W40, 3.57 ± 0.13; 101-1, 3.61 ± 0.14. *D*, a model of the induction of Cdc25A and Cdc25B degradation after nongenotoxic stress followed by G_2 arrest.

retardation can be explained at least in part by the simultaneous degradation of Cdc25A and Cdc25B (Fig. 2). Our results strongly suggest the presence of a nongenotoxic stress–dependent cell cycle checkpoint wherein Cdc25 phosphatases are degraded to down-regulate CDK activity. This checkpoint is mediated by stress-activated MAPKs, including p38 and JNK, as depicted in Fig. 6*D*. The proteasome inhibitor MG132 attenuated anisomycin-induced Cdc25B degradation, which strongly suggests that Cdc25B is degraded by the ubiquitin-proteasome pathway. Cdc25B is degraded in the steady state by the $SCF^{\beta\text{-}TrCP}$–mediated ubiquitinylation mechanism. It is unlikely that phosphorylation of S101 stimulated binding of $SCF^{\beta\text{-}TrCP}$ to the constitutive binding site, which is located more than 100 amino acids downstream of S101. It is necessary to identify the responsible ubiquitinylation system to understand JNK-mediated Cdc25B degradation more precisely.

Several reports have indicated a correlation between the malignancy of tumors and the overexpression of Cdc25A and Cdc25B (33, 34). Cdc25A and Cdc25B are oncogenic (35), and Cdc25A is a main target of the DNA damage checkpoint (1, 2, 34). Assuming that Cdc25B is a target of a nongenotoxic stress checkpoint, overexpression of Cdc25B may allow cells to become less sensitive to intrinsically harmful cell stresses that do not directly compromise genome integrity. Ignoring the detrimental stress signal, such as NaCl-induced distortion of the cytoskeleton by hyperosmolarity or anisomycin-induced inhibition of protein synthesis, may disrupt the proper regulation of chromosome segregation and cytokinesis during mitosis, which are well-known causative events of genome instability (36).

In conclusion, we have shown that Cdc25B is targeted for JNK-mediated degradation by cellular stress. The stress-induced checkpoint is initiated by the activation of JNK and p38, which phosphorylates Ser[101] of Cdc25B. This results in the rapid degradation of Cdc25B and cell cycle arrest.

Disclosure of Potential Conflicts of Interest

No potential conflicts of interest were disclosed.

Acknowledgments

Received 3/6/09; revised 4/22/09; accepted 6/3/09; published OnlineFirst 7/28/09.

Grant support: Long-range Research Initiative of the Japan Chemical Industry Association; Ministry of Health, Labor, and Welfare of Japan; Japan Society for the Promotion of Science; and Yamagiwa-Yoshida Fellowship from the International Union Against Cancer, Switzerland.

The costs of publication of this article were defrayed in part by the payment of page charges. This article must therefore be hereby marked *advertisement* in accordance with 18 U.S.C. Section 1734 solely to indicate this fact.

We thank Dr. H. Shima for the p38α plasmid and Dr. M. Ogata for information on the *sevenmaker* mutation of MAPKs.

References

1. Bartek J, Lukas J. Mammalian G_1- and S-phase checkpoints in response to DNA damage. Curr Opin Cell Biol 2001;13:738–47.
2. Busino L, Chiesa M, Draetta GF, Donzelli M. Cdc25A phosphatase: combinatorial phosphorylation ubiquitylation and proteolysis. Oncogene 2004;23:2050–6.
3. Mailand N, Podtelejnikov AV, Groth A, Mann M, Bartek J, Lukas J. Regulation of G_2/M events by Cdc25A through phosphorylation-dependent modulation of its stability. EMBO J 2002;21:5911–20.
4. Lindqvist A, Källström H, Lundgren A, Barsoum E, Rosenthal CK. Cdc25B cooperates with Cdc25A to induce mitosis but has a unique role in activating cyclin B1-Cdk1 at the centrosome. J Cell Biol 2005;171:35–45.
5. Bartek J, Lukas J. Chk1 and Chk2 kinases in checkpoint control and cancer. Cancer Cell 2003;3:421–9.
6. Jin J, Shirogane T, Xu L, et al. $SCF^{\beta\text{-}TRCP}$ links Chk1 signaling to degradation of the Cdc25A protein phosphatase. Genes Dev 2003;17:3062–74.
7. Chen MS, Hurov J, White LS, Woodford-Thomas T, Piwnica-Worms H. Absence of apparent phenotype in mice lacking Cdc25C protein phosphatase. Mol Cell Biol 2001;21:3853–61.
8. Ferguson AM, White LS, Donovan PJ, Piwnica-Worms H. Normal cell cycle and checkpoint responses in mice and cells lacking Cdc25B and Cdc25C protein phosphatases. Mol Cell Biol 2005;25:2853–60.
9. Lincoln AJ, Wickramasinghe D, Stein P, et al. Cdc25b phosphatase is required for resumption of meiosis during oocyte maturation. Nat Genet 2002;30:446–9.
10. Dutertre S, Cazales M, Quaranta M, et al. Phosphorylation of CDC25B by Aurora-A at the centrosome contributes to the G_2-M transition. J Cell Sci 2004;117:2523–31.
11. Kramer A, Mailand N, Lukas C, et al. Centrosome-associated Chk1 prevents premature activation of cyclin-B-Cdk1 kinase. Nat Cell Biol 2004;6:884–91.
12. Schmitt E, Boutros R, Froment C, Monsarrat B, Ducommun B, Dozier C. CHK1 phosphorylates CDC25B during the cell cycle in the absence of DNA damage. J Cell Sci 2006;119:4269–75.
13. Uchida S, Kuma A, Ohtsubo M, et al. Binding of 14-3-3β but not 14-3-3σ controls the cytoplasmic localization of CDC25B: binding site preferences of 14-3-3 subtypes and the subcellular localization of CDC25B. J Cell Sci 2004;117:3011–20.
14. Boutros R, Dozier C, Ducommun B. The when and where of CDC25 phosphatases. Curr Opin Cell Biol 2006;18:185–91.
15. Forrest A, Gabrielli B. Cdc25B activity is regulated by 14-3-3. Oncogene 2001;20:4393–401.
16. Davezac N, Baldin V, Gabrielli B, et al. Regulation of CDC25B phosphatases subcellular localization. Oncogene 2000;19:2179–85.
17. Johnson GL, Lapadat R. Mitogen-activated protein kinase pathways mediated by ERK JNK and p38 protein kinases. Science 2002;298:1911–2.
18. Manke IA, Nguyen A, Lim D, Stewart MQ, Elia AE, Yaffe MB. MAPKAP kinase-2 is a cell cycle checkpoint kinase that regulates the G_2/M transition and S phase progression in response to UV irradiation. Mol Cell 2005;17:37–48.
19. Bulavin DV, Amundson SA, Fornace AJ. p38 and Chk1 kinases: different conductors for the G_2/M checkpoint symphony. Curr Opin Genet Dev 2002;12:92–7.
20. Goloudina A, Yamaguchi H, Chervyakova DB, Appella E, Fornace AJ, Jr., Bulavin DV. Regulation of human Cdc25A stability by serine 75 phosphorylation is not sufficient to activate an S phase checkpoint. Cell Cycle 2003;2:473–8.
21. Goss VL, Cross JV, Ma K, Qian Y, Mola PW, Templeton DJ. SAPK/JNK regulates cdc2/cyclin B kinase through phosphorylation and inhibition of cdc25C. Cell Signal 2003;15:709–18.
22. Lindqvist A, Källström H, Karlsson-Rosenthal C. Characterisation of Cdc25B localisation and nuclear export during the cell cycle and in response to stress. J Cell Sci 2004;117:4979–90.
23. Uchida S, Ohtsubo M, Shimura M, et al. Nuclear export signal in CDC25B. Biochem Biophys Res Commun 2004;316:226–32.
24. Uchida S, Kubo A, Kizu R, et al. Amino acids C-terminal to the 14-3-3 binding motif in CDC25B affect the efficiency of 14-3-3 binding. J Biochem (Tokyo) 2006;139:761–9.
25. Bulavin DV, Higashimoto Y, Popoff IJ, et al. Initiation of a G_2/M checkpoint after ultraviolet radiation requires p38 kinase. Nature 2001;411:102–7.
26. Lemaire M, Froment C, Boutros R, et al. CDC25B phosphorylation by p38 and MK-2. Cell Cycle 2006;5:1649–53.
27. Rogakou EP, Pilch DR, Orr AH, Ivanova VS, Bonner WM. DNA double-stranded breaks induce histone H2AX phosphorylation on serine 139. J Biol Chem 1998;273:5858–68.
28. Cano E, Hazzalin CA, Mahadevan LC. Anisomycin-activated protein kinases p45 and p55 but not mitogen-activated protein kinases ERK-1 and -2 are implicated in the induction of c-fos and c-jun. Mol Cell Biol 1994;14:7352–62.
29. Iordanov MS, Pribnow D, Magun JL, et al. Ribotoxic stress response: activation of the stress-activated protein kinase JNK1 by inhibitors of the peptidyl transferase reaction and by sequence-specific RNA damage to the α-sarcin/ricin loop in the 28S rRNA. Mol Cell Biol 1997;17:3373–81.
30. Kanemori Y, Uto K, Sagata N. β-TrCP, recognizes a previously undescribed nonphosphorylated destruction motif in Cdc25A and Cdc25B phosphatases. Proc Natl Acad Sci U S A 2005;102:6279–84.
31. Hutter D, Chen O, Barnes J, Liu Y. Catalytic activation of mitogen-activated protein (MAP) kinase phosphatase-1 by binding to p38 MAP kinase: critical role of the p38 C-terminal domain in its negative regulation. Biochem J 2000;352:155–63.
32. Uto K, Inoue D, Shimuta K, Nakajo N, Sagata N. Chk1 but not Chk2 inhibits Cdc25 phosphatases by a novel common mechanism. EMBO J 2004;23:3386–96.
33. Kristjánsdóttir K, Rudolph J. Cdc25 phosphatases and cancer. Chem Biol 2004;11:1043–51.
34. Boutros R, Lobjois J, Ducommun B. CDC25 phosphatases in cancer cells: key players? Good targets? Nat Rev Cancer 2007;7:495–507.
35. Galaktionov K, Lee AK, Eckstein J, et al. CDC25 phosphatases as potential human oncogenes. Science 1995;269:1575–7.
36. Kops GJ, Weaver BA, Cleveland DW. On the road to cancer: aneuploidy and the mitotic checkpoint. Nat Rev Cancer 2005;5:773–85.

ARTICLE IN PRESS

Available online at www.sciencedirect.com

ScienceDirect

ELSEVIER

Biochemical and Biophysical Research Communications xxx (2007) xxx–xxx

BBRC

www.elsevier.com/locate/ybbrc

Decreased PARP-1 levels accelerate embryonic lethality but attenuate neuronal apoptosis in DNA polymerase β-deficient mice

Noriyuki Sugo [a,1], Naoko Niimi [a], Yasuaki Aratani [a], Mitsuko Masutani [b], Hiroshi Suzuki [c], Hideki Koyama [a,*]

[a] *Kihara Institute for Biological Research and Graduate School of Integrated Science, Yokohama City University, 641-12 Maioka-cho, Totsuka-ku, Yokohama 244-0813, Japan*

[b] *ADP-ribosylation in Oncology Project, National Cancer Research Institute, 1-1 Tsukiji 5-chome, Chuo-ku, Tokyo 104-0045, Japan*

[c] *National Research Center of Protozoa Diseases, Obihiro University of Agriculture and Veterinary Medicine, Nishi 2-13, Inada-cho, Obihiro, Hokkaido 080-8555, Japan*

Received 27 December 2006

Abstract

In mammalian cells, DNA polymerase β (Polβ) and poly(ADP-ribose) polymerase-1 (PARP-1) have been implicated in base excision repair (BER) and single-strand break repair. Polβ knockout mice exhibit extensive neuronal apoptosis during neurogenesis and die immediately after birth, while PARP-1 knockout mice are viable and display hypersensitivity to genotoxic agents and genomic instability. Although accumulating biochemical data show functional interactions between Polβ and PARP-1, such interactions in the whole animal have not yet been explored. To study this, we generate Polβ$^{-/-}$PARP-1$^{-/-}$ double mutant mice. Here, we show that the double mutant mice exhibit a profound developmental delay and embryonic lethality at mid-gestation. Importantly, the degree of the neuronal apoptosis was dramatically reduced in PARP-1 heterozygous mice in a Polβ null background. The reduction was well correlated with decreased levels of p53 phosphorylation at serine-18, suggesting that the apoptosis depends on the p53-mediated apoptosis pathway that is positively regulated by PARP-1. These results indicate that functional interactions between Polβ and PARP-1 play important roles in embryonic development and neurogenesis.

Keywords: DNA polymerase β; PARP-1; Knockout mouse; Development; Neuronal apoptosis

DNA repair is essential for maintaining the genome integrity for development and survival [1]. Base excision repair (BER) is the pathway for repair of DNA damage such as apurinic/apyrimidinic (AP) sites and base modifications, which spontaneously occur or are caused by a variety of endogenous and exogenous agents [2,3]. BER is initiated by monofunctional DNA glycosylases that remove a damaged base to generate an AP site, which is then excised by AP endonuclease 1 (APE1). This process is also carried out by bifunctional DNA glycosylases carrying APE1 activity. Then, the BER pathway is divided into the short-patch and long-patch subpathways, depending on the length of synthesized nucleotides and factors involved. DNA polymerase β (Polβ), one of the factors, plays a key role in BER. In the former subpathway, Polβ synthesizes one nucleotide to fill the gap and excises the 5′-dRP residue, followed by ligation with DNA ligase I (LIGI) or a XRCC1/LIGIII complex [3,4]. The latter subpathway synthesizes 2–10 nucleotides by Polβ and/or Polδ/ε with proliferating cell nuclear antigen (PCNA), displacing the damaged strand; the displaced strand is then excised by flap endonuclease 1 (FEN1), followed by ligation with LIGI [5].

Gu et al. [6] reported that Polβ knockout (Polβ$^{-/-}$) mice are embryonic lethal. We showed that Polβ-deficient embryos exhibit extensive apoptosis in newly generated

* Corresponding author. Fax: +81 45 820 1901.
E-mail address: koyama@yokohama-cu.ac.jp (H. Koyama).
[1] Present address: Graduate School of Frontier Biosciences, Osaka University, 1-3 Yamadaoka, Suita, Osaka 565-0871, Japan.

0006-291X/$ - see front matter © 2007 Elsevier Inc. All rights reserved.
doi:10.1016/j.bbrc.2006.12.230

post-mitotic neuronal cells in the developing central and peripheral nervous systems and that the mice die of respiratory failure immediately after birth [7]. We also showed that p53 deficiency can dramatically rescue the neuronal apoptosis, indicating involvement of the p53-dependent pathway in the apoptosis [8]. Polβ$^{-/-}$ mouse embryonic fibroblast (MEF) cells are viable and exhibit BER defects, as evidenced by increased sensitivity to DNA-alkylating agents [7,9]. However, the cells still retain an activity to repair damaged DNA bases *in vitro*, indicating that both the Polβ-dependent and -independent BER pathways are functioning *in vivo* [10].

Poly(ADP-ribose) polymerase-1 (PARP-1) is a nuclear localized protein that can be activated by DNA strand breaks [11]. The activated PARP-1 catalyzes the transfer of multiple ADP-ribose units to various nuclear proteins including histones and PARP-1 itself, using NAD^+ as a substrate. Synthesized poly(ADP-ribose) (PAR) is thought to act as a signal which regulates various cellular functions including DNA repair, cell cycle checkpoint control, chromatin remodeling, and carcinogenesis [11–13]. Recently, there is accumulating biochemical evidence showing that PARP-1 is directly involved in BER [14–16] as well as in single-strand break (SSB) repair [17,18]. That is, PARP-1 senses a SSB or BER intermediate (single nucleotide gap, SNG) in genomic DNA, binds to the damaged site, and catalyzes the auto-poly(ADP-ribosyl)ation. Then, the poly-ADP-ribosylated PARP-1 mediates efficient recruitment of XRCC1, LIGIII, and Polβ to the site and allows its repair via the short-patch subpathway [14,19,20]. Also, PARP-1 was reported to stimulate strand displacement during DNA synthesis by Polβ or Polδ/ε, in cooperation with FEN1 and PCNA, in the long-patch subpathway [16].

PARP-1 knockout (PARP-1$^{-/-}$) mice are viable and fertile [21–23], but the mice and their MEF cells display hypersensitivity to DNA-alkylating agents or γ-irradiation and genomic instability [17,21]. In PARP-1$^{-/-}$ MEF cells, the BER activity, assayed with cell-free extracts, was reported to be considerably impaired [14]. The data support the involvement of PARP-1 in BER, although contradictory data have also been reported [24].

PARP-1 can participates in signaling pathways leading to cell death. When cells suffer massive strand breaks, PARP-1 is fully activated, and a cellular NAD level is drastically reduced, resulting in cell death [25]. The same mechanism causes neuronal cell death in ischemia-reperfusion injury following cerebral ischemia [26]. PARP-1 mediates cell death by apoptosis-inducing factor (AIF), which triggers caspase-independent apoptosis [27]. These findings indicate that the level of PARP-1 activation by DNA damage is critical for stimulating the signaling pathways for cell death.

Dantzer et al. [14] reported that MEF cells lacking both Polβ and PARP-1 show a dramatic reduction in *in vitro* BER activity; however, they did not address the phenotypes of the embryos. In this study, we generate Polβ and PARP-1 double mutant mice and examine their phenotypes to explore potential interactions between Polβ and PARP-1 *in vivo*. We find that the double mutants exhibit earlier embryonic lethality than Polβ$^{-/-}$ single mutants. We also find that heterozygosity for PARP-1 dramatically reduces the neuronal apoptosis associated with Polβ deficiency. These results indicate critical functional interactions between the two proteins during embryonic development and neurogenesis.

Materials and methods

Mice. All mice, including mice heterozygous for either Polβ or PARP-1, were maintained as described previously [7,22]. Genotyping for the Polβ locus in animals or embryos was carried out by PCR, using a forward primer BP19 (5′-CCGTGCACAGGGACCTTCTG-3′) and two reverse primers: NSb3 (5′-CTGGTGAGTTAGCCTGAGAG-3′) for wild-type cells and KW2-2 (5′-GGCTACCCGTGATATTGCTGAA-3′) for mutant cells. PCR was performed in a reaction mixture (10 μl) containing 70 nM primers, 0.2 mM dNTPs, 0.25 U TaKaRa *Taq* DNA polymerase, 1 μl 10× PCR buffer (Mg^{2+} Plus) (Takara Bio Co.), and genomic DNA. After denaturing at 95 °C for 5 min, the mixture was incubated 38 times for 1 min each at 95 °C, at 58 °C, and at 72 °C, followed by a 7-min extension at 72 °C. The product was electrophoresed in a 1% agarose gel and stained with ethidium bromide. The diagnostic bands were 1.1 and 1.4 kbp for wild-type and mutant cells, respectively. Genotyping for the PARP-1 locus was carried out using a forward primer mp66S (5′-AAACCGACA CGTTAGCGGAG-3′) and a reverse primer mp23A (5′-CTTGGGAATA CTCTCGCTGC-3′). PCR was performed in the same manner as above, except for 300 nM primers in a reaction mixture and electrophoresis in a 2% gel. The bands diagnostic for wild-type and mutant cells were 156 bp and 1.25 kbp, respectively.

Histology and immunohistochemistry. Embryonic brain sections for histological analysis were prepared as described previously [7]. The sections were incubated with rabbit anti-cleaved caspase-3 polyclonal antibody (Cell Signaling Technology; 1:100). Horseradish peroxidase (HRP)-conjugated antibody (Chemicon) was used for a secondary antibody to visualize the primary antibody.

Western blot analysis. Whole cell extracts were prepared from developing telencephalons in E13.5 embryos, subjected to sodium dodesylsulfate–polyacrylamide gel electrophoresis (SDS–PAGE). Aliquots of the extracts (30 μg protein) were electrophoresed in an 8.0% or 12% polyacrylamide gel, and transferred to an Immobilon (Millipore) or Immunblot membrane (Bio-Rad) as described [7]. The membrane was blocked with 1% skim-milk/TBST and probed with various antibodies: anti-human phospho-p53 (Ser-15) antibody (Cell Signaling Technology; 1:1000), anti-Polβ monoclonal antibody (Labvision; 1:1000), anti-XRCC1 polyclonal antibody (Santa Cruz; 1:1000), anti-PARP-1 polyclonal antibody (Biomol; 1:1000), anti-cleaved caspase-3 polyclonal antibody (Cell Signaling Technology; 1:1000), and anti-PAR monoclonal antibody (Alexis; 1:1000), in 1% BSA/TBST. Signals were detected with HRP-conjugated secondary antibody (Nacalai Tesque) and chemiluminescent detection reagents (ECL Plus Kit, Amersham).

Results

Polβ and PARP-1 double mutant embryos die at mid-gestation

We crossed Polβ$^{+/-}$ and PARP-1$^{+/-}$ mice and the resulting doubly heterozygous Polβ$^{+/-}$PARP-1$^{+/-}$ mice developed normally and were fertile (data not shown). Next, the heterozygous mice were intercrossed, and the breeding data are summarized in Table 1. Among the offspring, Polβ$^{-/-}$PARP-1$^{-/-}$ double mutant embryos at

Please cite this article in press as: N. Sugo et al., Decreased PARP-1 levels accelerate embryonic lethality but attenuate ..., Biochem. Biophys. Res. Commun. (2007), doi:10.1016/j.bbrc.2006.12.230

Table 1
Genotypic analysis of Polβ$^{+/-}$PARP-1$^{+/-}$ intercrosses

Age	No. of mice with genotype									Total no. of litters	Total no. of mice
	Polβ$^{+/+}$			Polβ$^{+/-}$			Polβ$^{-/-}$				
	PARP-1			PARP-1			PARP-1				
	+/+	+/−	−/−	+/+	+/−	−/−	+/+	+/−	−/−		
E9.5	1	2	1	4	6	8	4	7	1	4	34
E10.5–11.5	6	16	9	8	24	25	6	16	4	11	114
E13.5	1	5	2	14	24	7	2	6	0	9	61
E18.5	1	5	6	3	14	5	2	4	0	5	40
4 weeks	3	8	1	21	17	5	0	0	0	10	55

The number of live embryos and mice of each genotype at the indicated stages is shown.

E9.5 displayed a profound developmental delay compared to the littermates with other genotypes (see Fig. 1A). At E10.5, the developmental stage of the double mutants proceeded; the embryos were much smaller than a Polβ$^{-/-}$ PARP-1$^{+/+}$ littermate (Fig. 1B), although particular malformations were undetected. The double mutants were alive around E11.5, but eventually died and resorbed *in utero* by E13.5 (Table 1). These phenotypes were considerably different from those in either Polβ$^{-/-}$ or PARP-1$^{-/-}$ single mutant, which can proliferate without showing apparently retarded growth during embryogenesis [7,21,23]. On the other hand, Polβ$^{+/-}$PARP-1$^{+/+}$ and Polβ$^{+/+}$PARP-1$^{+/-}$ mice survived and were fertile as reported [7,21,23]; Polβ$^{+/-}$PARP-1$^{-/-}$ mice, like Polβ$^{+/+}$PARP-1$^{-/-}$ mice, were born normally and developed into adulthood. Moreover, Polβ$^{-/-}$PARP-1$^{+/-}$ mice, like Polβ$^{-/-}$ mice [7], developed during the whole embryonic stage but died just after birth, although the mice were born at nearly the predicted Mendelian frequency (Table 1 and data not shown). These results indicate that physiological interactions between Polβ and PARP-1 play indispensable roles in embryonic development.

Polβ and PARP-1 deficiency affect neuronal apoptosis in an opposite way

To examine whether PARP-1 deficiency affected neuronal apoptosis, we carried out an immunohistochemical analysis using anti-cleaved caspase-3 antibody, a useful marker for detecting apoptotic cells [8]. We stained sections of developing telencephalons in E13.5 embryos with different genotypes. As compared to wild-type controls (Fig. 2A), in Polβ$^{-/-}$PARP-1$^{+/+}$ brains (Fig. 2B), a large number of cleaved caspase-3-positive (stained) cells were observed in areas of medial ganglionic eminence (MGE), lateral ganglionic eminence (LGE), and neocortex (NCX). Importantly, in Polβ$^{-/-}$PARP-1$^{+/-}$ brains (Fig. 2C), such stained cells dramatically decreased, indicating that heterozygosity for the PARP-1 gene in a Polβ null background can remarkably rescue the neuronal apoptosis. In addition, Polβ$^{+/-}$PARP-1$^{-/-}$ brains (Fig. 2D), like wild-type and Polβ$^{+/+}$PARP-1$^{-/-}$ brains (data not shown), showed almost no apoptotic cells. We failed to examine the apoptosis in brains of Polβ$^{-/-}$PARP-1$^{-/-}$ double mutants, because their embryos died by E13.5.

PARP-1 levels correlate with the extent of neuronal apoptosis

Physical and functional interactions of PARP-1 with BER proteins have been reported [14,19,20]. We examined the levels of PARP-1, Polβ and XRCC1 in whole cell extracts prepared from E13.5 telencephalones of wild-type and mutant mice, by Western blotting using the corresponding antibodies. As shown in Fig. 3A, PARP-1 levels in Polβ$^{-/-}$ PARP-1$^{+/+}$ extract were ~2-fold less than that in wild-type

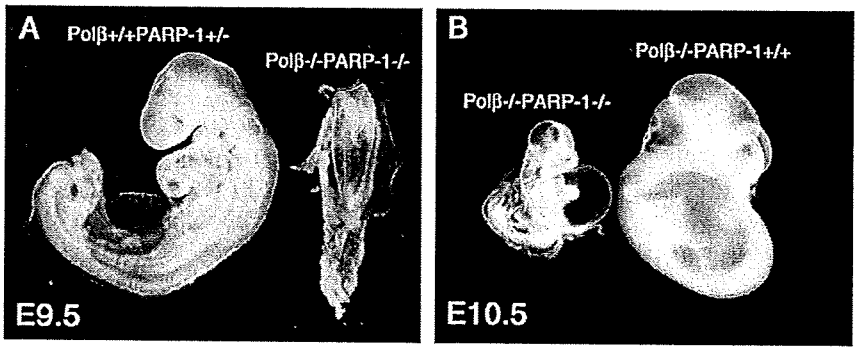

Fig. 1. Morphology of developing mouse embryos. (A) Whole view of a Polβ$^{-/-}$PARP$^{-/-}$ embryo at E9.5, displaying a severe developmental delay compared to a Polβ$^{+/+}$PARP$^{+/-}$ littermate. (B) Whole view of a Polβ$^{-/-}$PARP-1$^{-/-}$ embryo at E10.5, which is much smaller than a Polβ$^{-/-}$PARP$^{+/+}$ littermate.

Please cite this article in press as: N. Sugo et al., Decreased PARP-1 levels accelerate embryonic lethality but attenuate ..., Biochem. Biophys. Res. Commun. (2007), doi:10.1016/j.bbrc.2006.12.230

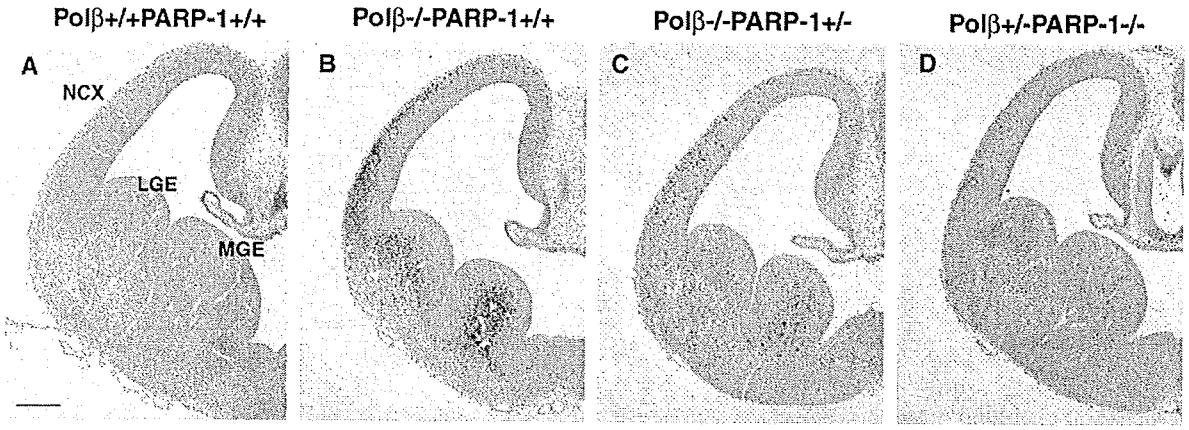

Fig. 2. Neuronal apoptosis observed in wild-type and mutant brains with different genotypes. Coronal sections of E13.5 developing telencephalons in: (A) $Polβ^{+/+}PARP\text{-}1^{+/+}$ (wild-type), (B) $Polβ^{-/-}PARP\text{-}1^{+/+}$, (C) $Polβ^{-/-}PARP\text{-}1^{+/-}$, and (D) $Polβ^{+/-}PARP\text{-}1^{-/-}$ mice were immunohistochemically stained with anti-cleaved caspase-3 antibody. LGE, lateral ganglionic eminence; MGE, medial ganglionic eminence; NCX, neocortex. Scale bar, 200 μm.

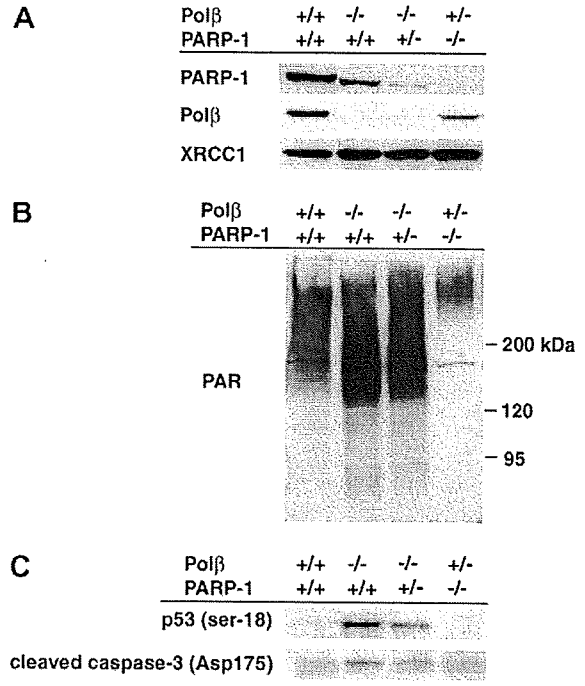

Fig. 3. Western blot analysis of whole cell extracts prepared from wild-type and mutant telencephalons with different genotypes. Aliquots of cell extracts were analyzed by SDS–PAGE, followed by immunoblotting using the corresponding antibodies, as described in Materials and methods. (A) Levels of PARP-1, Polβ and XRCC1 in cell extracts from E13.5 telencephalons of $Polβ^{+/+}PARP\text{-}1^{+/+}$ (wild-type), $Polβ^{-/-}PARP\text{-}1^{+/+}$, $Polβ^{-/-}PARP\text{-}1^{+/-}$, and $Polβ^{+/-}PARP\text{-}1^{-/-}$ mice. The bands of XRCC1 confirm equal loading of the extracts. (B) Poly(ADP-ribosyl)ated proteins in the same extracts used in (A). (C) Levels of 53 phosphorylation at serine-18 and cleaved caspase-3 in the same extracts used in (A).

controls, suggesting that PARP-1 expression was likely influenced by the Polβ level. Except for this control level, PARP-1 was produced in a gene dosage-dependent manner. That is, compared to the $Polb^{-/-}PARP\text{-}1^{+/+}$ extract, PARP-1 protein was extremely decreased in $Polb^{-/-}PARP\text{-}1^{+/-}$ extract and undetectable in $Polβ^{+/-}PARP\text{-}1^{-/-}$ extract. As expected, Polβ protein was absent in both $Polβ^{-/-}PARP\text{-}1^{+/+}$ and $Polβ^{-/-}PARP\text{-}1^{+/-}$extracts. There was no significant difference in XRCC1 expression among the mice examined (Fig. 3A). Taken together with the data in Fig. 2, it is evident that, in Polβ null brains, the extent of the neuronal apoptosis is well correlated with the level of PARP-1.

To study whether PAR was associated with neuronal apoptosis, we examined PAR levels in the same cell extracts using anti-PAR antibody (Fig. 3B). The levels of PAR in $Polβ^{-/-}PARP\text{-}1^{+/+}$ and $Polβ^{-/-}PARP\text{-}1^{+/-}$ extracts were roughly the same, but seemed to be a little greater than that in wild-type controls. In $Polβ^{+/-}PARP\text{-}1^{-/-}$ extract, the PAR level reduced markedly but not completely, probably because the residual PAR was synthesized by PARP-2 having a catalytic activity similar to PARP-1 [28]. These results indicate that the degree of the apoptosis shown in Fig. 2 is independent from the PAR levels, suggesting no direct involvement of the PAR signaling in the neuronal apoptosis arising in Polβ null mice.

PARP-1 positively regulates the p53-dependent apoptosis pathway

We reported that the neuronal apoptosis is mediated by the phosphorylation of serine-18 of p53 protein [8]. Interactions between p53 and PARP-1 have been observed in the DNA damage-responsive signaling pathways [29,30]. To study whether PARP-1 influenced p53 transactivation, we examined p53 phosphorylation in the extracts of E13.5 telencephalons used above (Fig. 3A), using anti-human phospho-p53 (Ser-15) antibody (the Ser-15 of human p53 is equivalent to the Ser-18 of mouse p53). The serine-18 in $Polβ^{-/-}PARP\text{-}1^{+/+}$ extract was markedly phosphorylated compared to wild-type controls, as described previously [8]. Importantly, the phosphorylation level in $Polβ^{-/-}PARP\text{-}1^{+/-}$ extract obviously decreased to approximately

one-half of that found in Polβ$^{-/-}$PARP-1$^{+/+}$ extract, and the signal was absent in Polβ$^{+/-}$PARP-1$^{-/-}$ (Fig. 3C) and Polβ$^{+/+}$PARP-1$^{-/-}$ extracts (data not shown). Taken together with the data in Fig. 3A, these results clearly indicate that the p53 phosphorylation at serine-18 correlates with the levels of PARP-1 expression depending on gene dosage. We also examined cleaved caspase-3 levels by Western blotting. Notably, the cleaved caspase-3 levels clearly paralleled the levels of p53 phosphorylation (Fig. 3C). Consistent with the immunostaining data in Fig. 2, Polβ$^{-/-}$PARP-1$^{+/+}$ extract revealed a strongly positive band of cleaved caspase-3, but Polβ$^{-/-}$PARP-1$^{+/-}$ extract revealed an obviously lower expression. In Polβ$^{+/-}$PARP-1$^{-/-}$ extract, the signal was hardly seen as in wild-type controls. These results strongly suggest that PARP-1 positively regulates the p53-dependent pathway in the neuronal apoptosis associated with Polβ deficiency.

Discussion

Mice doubly deficient in Polβ and PARP-1 were lethal at mid-gestation. The reduction of PARP-1 expression in a Polβ null or heterozygous background caused a marked decrease in neuronal apoptosis in embryonic brains. These observations obviously show important physiological interactions between Polβ and PARP-1 proteins in embryonic development and neurogenesis.

Polβ$^{-/-}$PARP-1$^{-/-}$ mutant mice revealed a severe developmental delay around E10.5 and resulted in death by E13.5 (Fig. 1 and Table 1). It has been shown that Polβ$^{-/-}$ mice die immediately after birth [7,8], while PARP-1$^{-/-}$ mice can survive and fertile [21,23]. Therefore, our present observations indicate the acceleration of lethality associated with Polβ deficiency by PARP-1 inactivation. Polβ and PARP-1 are thought to cooperatively function in the process of SSB repair [17,18] and BER [14–16]. In developing embryos, SSBs may be generated spontaneously or by direct excision of a DNA backbone by endogenous agents [1]. Also, a large number of AP sites or other base lesions would arise spontaneously and be processed in the BER pathway, generating SNGs [2,3,31]. Given crucial roles for Polβ in BER, Polβ deficiency would greatly retard the repair of the damage, leading to the accumulation of unrepaired breaks [8,32]. PARP-1 binds to the damage and becomes auto-poly(ADP-ribosyl)ated; the activated PARP-1 enhances access of BER proteins to the damaged site to complete the repair process [14–16]. However, PARP-1 deficiency, which caused a drastic, but not complete, loss of PAR (see Fig. 3B), would retard the process as shown in PARP-1$^{-/-}$ MEF cells [28]. Moreover, double deficiency of Polβ and PARP-1 would result in further retardation as described [14]; consequently, some of the unrepaired breaks could be altered to more cytotoxic DBSs, when replication forks run into the breaks during S phase and collapse [33]. The increasing amounts of these strand breaks would cause severe defects in transcription and DNA replication, eventually leading to growth arrest, cell death, and lethality of the animal [34]. Thus, we conclude that a functional cooperation of Polβ and PARP-1 is indispensable for survival and embryonic development.

PARP-1 protein in cell extracts from E13.5 telencephalons in mice with distinct genotypes was expressed in a gene dosage-dependent manner (Fig. 3A). Importantly, the extent of the neuronal apoptosis caused by Polβ deficiency (Fig. 2) was well correlated with the PARP-1 levels. Notably, heterozygosity for PARP-1 in Polβ$^{-/-}$ mice dramatically suppressed the apoptosis. In contrast, no correlation was found between the extent of the apoptosis (Fig. 2) and the PAR levels (Fig. 3B). These results suggest that PARP-1 itself controls the neuronal apoptosis. Similarly, the phosphorylation level of p53 at serine-18 correlated well with the degree of the apoptosis in a Polβ$^{-/-}$ background (Fig. 3C); importantly, the phosphorylation level was significantly reduced in Polβ$^{-/-}$PARP$^{+/-}$ mice compared to that in Polβ$^{-/-}$PARP-1$^{+/+}$ littermates. This result also suggests that PARP-1 positively regulates p53 phosphorylation in developing brains, thereby controlling the neuronal apoptosis. Collectively, it is evident that both PARP-1 and p53 are cooperatively involved in the process of the neuronal apoptosis associated with Polβ deficiency.

How does PARP-1 interact with p53 in the process of the neuronal apoptosis? As noted above, in developing brains, Polβ and PARP-1 deficiency would cause severe defects in repair of SSBs and SNGs and leave unrepaired breaks, thereby generating DSBs. In response to these breaks, ataxia-telangiectasia mutated (ATM), a key player serving in cell cycle checkpoint response and apoptosis, would be activated and phosphorylate p53 protein [35]. However, the present data show that reduction or loss of PARP-1 activity in a Polβ$^{-/-}$ background significantly lowered the p53 phosphorylation levels (Fig. 3A and C). It may be possible that PARP-1 positively regulates the ATM-p53 signaling pathway, through which p53 is phosphorylated to act as a downstream signal for cell cycle checkpoint and apoptosis. Thus, PARP-1 defect would cause a reduced transactivation of p53, leading to a striking decrease in neuronal apoptosis as seen in Fig. 2. Our finding resembles the observation reported by Wieler et al. [30], who showed that in human breast adenocarcinoma and fibrobalst cell lines, PARP-1 inhibition causes a marked disruption of p53-mediated G1 arrest following ionizing radiation, and suggested that PARP-1 is a positive regulator of the p53-mediated G1 arrest response. In contrast, our finding seems to be inconsistent with the results that PARP-1 negatively regulates ATM kinase activity for p53, since p53 phosphorylation is augmented in PARP-1 null MEF cells treated with neocarzinostatin, an anti-tumor agent that can induce DSBs [36]. Although the reason for the differences is not known, ATM response to DNA damage endogenously arising in developing brains defective in Polβ and PARP-1 might differ from that induced in the drug-treated mutant MEF cells. Further study should be needed to clarify the role for the interactions of the proteins in embryogenesis and neurogenesis.

Please cite this article in press as: N. Sugo et al., Decreased PARP-1 levels accelerate embryonic lethality but attenuate ..., Biochem. Biophys. Res. Commun. (2007), doi:10.1016/j.bbrc.2006.12.230

Acknowledgments

We thank F. Oonuma for animal care. N.S. is a recipient of Research Fellowship of the Japan Society for the Promotion of Science for Young Scientists. This work was supported in part by Grant-in-Aid for Scientific Research from the Ministry of Education, Culture, Spots, Science, and Technology of Japan.

References

[1] T. Lindahl, R.D. Wood, Quality control by DNA repair, Science 286 (1999) 1897–1905.
[2] D.E. Barnes, T. Lindahl, Repair and genetic consequences of endogenous DNA base damage in mammalian cells, Annu. Rev. Genet. 38 (2004) 445–476.
[3] S.H. Wilson, Mammalian base excision repair and DNA polymerase beta, Mutat. Res. 407 (1998) 203–215.
[4] J.L. Parsons, I.I. Dianova, S.L. Allinson, G.L. Dianov, DNA polymerase beta promotes recruitment of DNA ligase IIIalpha-XRCC1 to sites of base excision repair, Biochemistry 44 (2005) 10613–10619.
[5] A. Klungland, T. Lindahl, Second pathway for completion of human DNA base excision-repair: reconstitution with purified proteins and requirement for DNase IV (FEN1), EMBO J. 16 (1997) 3341–3348.
[6] H. Gu, J.D. Marth, P.C. Orban, H. Mossmann, K. Rajewsky, Deletion of a DNA polymerase beta gene segment in T cells using cell type-specific gene targeting, Science 265 (1994) 103–106.
[7] N. Sugo, Y. Aratani, Y. Nagashima, Y. Kubota, H. Koyama, Neonatal lethality with abnormal neurogenesis in mice deficient in DNA polymerase beta, EMBO J. 19 (2000) 1397–1404.
[8] N. Sugo, N. Niimi, Y. Aratani, K. Takiguchi-Hayashi, H. Koyama, p53 deficiency rescues neuronal apoptosis but not differentiation in DNA polymerase beta-deficient mice, Mol. Cell. Biol. 24 (2004) 9470–9477.
[9] R.W. Sobol, J.K. Horton, R. Kuhn, H. Gu, R.K. Singhal, R. Prasad, K. Rajewsky, S.H. Wilson, Requirement of mammalian DNA polymerase-beta in base-excision repair, Nature 379 (1996) 183–186, published errata appear in Nature 379(6568) (1996) 848; 383(6599) (1996) 457.
[10] S. Biade, R.W. Sobol, S.H. Wilson, Y. Matsumoto, Impairment of proliferating cell nuclear antigen-dependent apurinic/apyrimidinic site repair on linear DNA, J. Biol. Chem. 273 (1998) 898–902.
[11] V. Schreiber, F. Dantzer, J.C. Ame, G. de Murcia, Poly(ADP-ribose): novel functions for an old molecule, Nat. Rev. Mol. Cell. Biol. 7 (2006) 517–528.
[12] M. Masutani, H. Nakagama, T. Sugimura, Poly(ADP-ribose) and carcinogenesis, Genes Chromosomes Cancer 38 (2003) 339–348.
[13] V. Pirrotta, Transcription puffing with PARP, Science 299 (2003) 528–529.
[14] F. Dantzer, G. de La Rubia, J. Menissier-De Murcia, Z. Hostomsky, G. de Murcia, V. Schreiber, Base excision repair is impaired in mammalian cells lacking Poly(ADP-ribose) polymerase-1, Biochemistry 39 (2000) 7559–7569.
[15] J.L. Parsons, I.I. Dianova, S.L. Allinson, G.L. Dianov, Poly(ADP-ribose) polymerase-1 protects excessive DNA strand breaks from deterioration during repair in human cell extracts, FEBS J. 272 (2005) 2012–2021.
[16] R. Prasad, O.I. Lavrik, S.J. Kim, P. Kedar, X.P. Yang, B.J. Vande Berg, S.H. Wilson, DNA polymerase beta -mediated long patch base excision repair. Poly(ADP-ribose)polymerase-1 stimulates strand displacement DNA synthesis, J. Biol. Chem. 276 (2001) 32411–32414.
[17] C. Trucco, F.J. Oliver, G. de Murcia, J. Menissier-de Murcia, DNA repair defect in poly(ADP-ribose) polymerase-deficient cell lines, Nucleic Acids Res. 26 (1998) 2644–2649.
[18] S. Okano, L. Lan, K.W. Caldecott, T. Mori, A. Yasui, Spatial and temporal cellular responses to single-strand breaks in human cells, Mol. Cell. Biol. 23 (2003) 3974–3981.
[19] K.W. Caldecott, S. Aoufouchi, P. Johnson, S. Shall, XRCC1 polypeptide interacts with DNA polymerase beta and possibly poly (ADP-ribose) polymerase, and DNA ligase III is a novel molecular 'nick-sensor' in vitro, Nucleic Acids Res. 24 (1996) 4387–4394.
[20] J.B. Leppard, Z. Dong, Z.B. Mackey, A.E. Tomkinson, Physical and functional interaction between DNA ligase IIIalpha and poly(ADP-Ribose) polymerase 1 in DNA single-strand break repair, Mol. Cell. Biol. 23 (2003) 5919–5927.
[21] J.M. de Murcia, C. Niedergang, C. Trucco, M. Ricoul, B. Dutrillaux, M. Mark, F.J. Oliver, M. Masson, A. Dierich, M. LeMeur, C. Walztinger, P. Chambon, G. de Murcia, Requirement of poly(ADP-ribose) polymerase in recovery from DNA damage in mice and in cells, Proc. Natl. Acad. Sci. USA 94 (1997) 7303–7307.
[22] M. Masutani, H. Suzuki, N. Kamada, M. Watanabe, O. Ueda, T. Nozaki, K. Jishage, T. Watanabe, T. Sugimoto, H. Nakagama, T. Ochiya, T. Sugimura, Poly(ADP-ribose) polymerase gene disruption conferred mice resistant to streptozotocin-induced diabetes, Proc. Natl. Acad. Sci. USA 96 (1999) 2301–2304.
[23] Z.Q. Wang, B. Auer, L. Stingl, H. Berghammer, D. Haidacher, M. Schweiger, E.F. Wagner, Mice lacking ADPRT and poly(ADP-ribosyl)ation develop normally but are susceptible to skin disease, Genes Dev. 9 (1995) 509–520.
[24] M.D. Vodenicharov, F.R. Sallmann, M.S. Satoh, G.G. Poirier, Base excision repair is efficient in cells lacking poly(ADP-ribose) polymerase 1, Nucleic Acids Res. 28 (2000) 3887–3896.
[25] L. Virag, Structure and function of poly(ADP-ribose) polymerase-1: role in oxidative stress-related pathologies, Curr. Vasc. Pharmacol. 3 (2005) 209–214.
[26] M.J. Eliasson, K. Sampei, A.S. Mandir, P.D. Hurn, R.J. Traystman, J. Bao, A. Pieper, Z.Q. Wang, T.M. Dawson, S.H. Snyder, V.L. Dawson, Poly(ADP-ribose) polymerase gene disruption renders mice resistant to cerebral ischemia, Nat. Med. 3 (1997) 1089–1095.
[27] S.W. Yu, H. Wang, M.F. Poitras, C. Coombs, W.J. Bowers, H.J. Federoff, G.G. Poirier, T.M. Dawson, V.L. Dawson, Mediation of poly(ADP-ribose) polymerase-1-dependent cell death by apoptosis-inducing factor, Science 297 (2002) 259–263.
[28] W.M. Shieh, J.C. Ame, M.V. Wilson, Z.Q. Wang, D.W. Koh, M.K. Jacobson, E.L. Jacobson, Poly(ADP-ribose) polymerase null mouse cells synthesize ADP-ribose polymers, J. Biol. Chem. 273 (1998) 30069–30072.
[29] C.M. Simbulan-Rosenthal, D.S. Rosenthal, R. Luo, M.E. Smulson, Poly(ADP-ribosyl)ation of p53 during apoptosis in human osteosarcoma cells, Cancer Res. 59 (1999) 2190–2194.
[30] S. Wieler, J.P. Gagne, H. Vaziri, G.G. Poirier, S. Benchimol, Poly(ADP-ribose) polymerase-1 is a positive regulator of the p53-mediated G1 arrest response following ionizing radiation, J. Biol. Chem. 278 (2003) 18914–18921.
[31] C. Cistulli, O.I. Lavrik, R. Prasad, E. Hou, S.H. Wilson, AP endonuclease and poly(ADP-ribose) polymerase-1 interact with the same base excision repair intermediate, DNA Repair (Amst) 3 (2004) 581–591.
[32] N. Niimi, N. Sugo, Y. Aratani, H. Koyama, Genetic interaction between DNA polymerase beta and DNA-PKcs in embryogenesis and neurogenesis, Cell Death Differ. 12 (2005) 184–191.
[33] N. Saleh-Gohari, H.E. Bryant, N. Schultz, K.M. Parker, T.N. Cassel, T. Helleday, Spontaneous homologous recombination is induced by collapsed replication forks that are caused by endogenous DNA single-strand breaks, Mol. Cell. Biol. 25 (2005) 7158–7169.
[34] B.S. Heyer, A. MacAuley, O. Behrendtsen, Z. Werb, Hypersensitivity to DNA damage leads to increased apoptosis during early mouse development, Genes Dev. 14 (2000) 2072–2084.
[35] Y. Shiloh, ATM and related protein kinases: safeguarding genome integrity, Nat. Rev. Cancer 3 (2003) 155–168.
[36] F. Watanabe, H. Fukazawa, M. Masutani, H. Suzuki, H. Teraoka, S. Mizutani, Y. Uehara, Poly(ADP-ribose) polymerase-1 inhibits ATM kinase activity in DNA damage response, Biochem. Biophys. Res. Commun. 319 (2004) 596–602.

Please cite this article in press as: N. Sugo et al., Decreased PARP-1 levels accelerate embryonic lethality but attenuate ..., Biochem. Biophys. Res. Commun. (2007), doi:10.1016/j.bbrc.2006.12.230

Available online at www.sciencedirect.com
ScienceDirect
Biochemical and Biophysical Research Communications 355 (2007) 451–456
BBRC
www.elsevier.com/locate/ybbrc

Poly(etheno ADP-ribose) blocks poly(ADP-ribose) glycohydrolase activity

Masayasu Shirato [a,b,c,1], Shunichi Tozawa [a,c,1], Daisuke Maeda [a], Masatoshi Watanabe [c], Hitoshi Nakagama [b], Mitsuko Masutani [a,b,*]

[a] *ADP-ribosylation in Oncology Project, National Cancer Center Research Institute, 5-1-1, Tsukiji, Chuo-ku, Tokyo 104-0045, Japan*
[b] *Biochemistry Division, National Cancer Center Research Institute, 5-1-1, Tsukiji, Chuo-ku, Tokyo 104-0045, Japan*
[c] *Division of Materials Science and Chemical Engineering, Graduate School of Engineering, Yokohama National University, 79-5 Tokiwadai, Hodogaya-ku, Yokohama 240-8501, Japan*

Received 25 January 2007
Available online 8 February 2007

Abstract

Poly(ADP-ribose) is a biopolymer synthesized by poly(ADP-ribose) polymerases. Recent findings suggest the possibility for modulation of cellular functions including cell death and mitosis by poly(ADP-ribose). Derivatization of poly(ADP-ribose) may be useful for investigating the effects of poly(ADP-ribose) on various cellular processes. We prepared poly(etheno ADP-ribose) (poly(εADP-ribose)) by converting the adenine moiety of poly(ADP-ribose) to 1-N^6-etheno adenine residues. Poly(εADP-ribose) is shown to be highly resistant to digestion by poly(ADP-ribose) glycohydrolase (Parg). On the other hand, poly(εADP-ribose) could be readily digested by phosphodiesterase. Furthermore, poly(εADP-ribose) inhibited Parg activity to hydrolyse ribose–ribose bonds of poly(ADP-ribose). This study suggests the possibility that poly(εADP-ribose) might be a useful tool for studying the poly(ADP-ribose) dynamics and function of Parg. This study also implies that modification of the adenine moiety of poly(ADP-ribose) abrogates the susceptibility to digestion by Parg.

Keywords: Poly(ADP-ribose) glycohydrolase; Poly(etheno ADP-ribose); Poly(ADP-ribose); Inhibitor

The poly(ADP-ribosylation) reaction is catalyzed by poly(ADP-ribose) polymerases (Parps) using NAD as a substrate on various acceptor molecules, including histones and Parps [1–4]. Phosphodiesterase (PDE) degrades poly(ADP-ribose) to 5″-phosphoribosyl-5′-AMP (PR-AMP) and 5′-AMP [5]. In intact cells, poly(ADP-ribose) is mainly degraded to ADP-ribose by poly(ADP-ribose) glycohydrolase (Parg) [6,7]. This degradation reaction of poly(ADP-ribose) is involved in DNA damage responses [8–11], transcription [12] and chromatin remodeling [13]. Poly(ADP-ribose) so formed in cells is highly enriched in metaphase chromosomes, and injection of Parg into intact cells resulted in disturbed chromosome segregation [14]. Accumulation of poly(ADP-ribose) in nuclei also induces cell death in neuronal cells [15,16]. It is also reported that Parg inhibitor enhances sensitivities of cancer cells to anti-cancer drug [17].

Poly(ADP-ribose) synthesis and degradation appear to be dynamically controlled in the cells [18,19]; thus, poly(ADP-ribose) derivatives, which are resistant to degradation by Parg within the cells, might be useful for the study of poly(ADP-ribose) function. Oei et al. prepared poly(ADP-ribose) containing 1-N^6-etheno adenine (εA) moieties and reported that the modified poly(ADP-ribose) is digestable by Parg [20]. In their preparation, the conversion percentage of adenine moieties to εA moieties seemed to be less than optimal. Here, we prepared poly(εADP-ribose) with almost complete conversion of

* Corresponding author. Present address: ADP-ribosylation in Oncology Project, National Cancer Center Research Institute, 1-1 Tsukiji 5-chome, Chuo-ku, Tokyo 104-0045, Japan. Fax: +81 3 3542 2530.
E-mail address: mmasutan@gan2.res.ncc.go.jp (M. Masutani).
[1] These authors contributed equally to this work.

0006-291X/$ - see front matter © 2007 Elsevier Inc. All rights reserved.
doi:10.1016/j.bbrc.2007.01.171

adenine moieties in poly(ADP-ribose) to εA moieties (Fig. 1), and demonstrated that poly(εADP-ribose) is resistant to Parg activity. We further showed that Parg activity is inhibited by poly(εADP-ribose).

Materials and methods

Preparation of poly(εADP-ribose). Poly(ADP-ribose) was prepared using *E. coli* expressing recombinant human PARP-1 [21]. Average chain length was estimated to be around 13 ADP-ribose residues [22]. One hundred micrograms of poly(ADP-ribose) was mixed with 0.1 M chloroacetaldehyde (Tokyo Kasei) and 0.2 M ammonium acetate in a volume of 1.0 ml and reacted at 60 °C for 4 h. The reaction was stopped by adding ammonium solution to 0.8% (v/v) and after precipitation with ethanol, poly(εADP-ribose) was dissolved in H_2O and the amount was measured by UV absorbance at 275 nm in 100 mM potassium phosphate buffer (pH 7.0) using ε_{275} value of 6000, which was reported for 1-N^6-etheno adenosine [23].

^{32}P-labelled poly(εADP-ribose) at 5′-AMP moieties was prepared using ^{32}P-poly(ADP-ribose) [21]. The chain length of ^{32}P-poly(ADP-ribose) was between 3 and 15 ADP-ribose residues.

Digestion of poly(εADP-ribose) by PDE and Parg activities. Poly(εADP-ribose) or poly(ADP-ribose) was incubated with rat Parg fused with glutathione-*S*-transferase (GST-Parg) [21] in a reaction mixture containing 20 mM potassium phosphate (pH 7.5), 0.05% Triton X-100, and 10 mM β-mercaptoethanol at 25 °C for 2 h. Poly(εADP-ribose) or poly(ADP-ribose) was incubated with 0.004 U of snake venom PDE (Worthington) [24] in a reaction mixture containing 10 mM sodium phosphate (pH 7.0), 10 mM $MgCl_2$ at 37 °C for 2 h. Sf9 cells expressing full-length rat Parg using baculovirus system (Bac to Bac System,

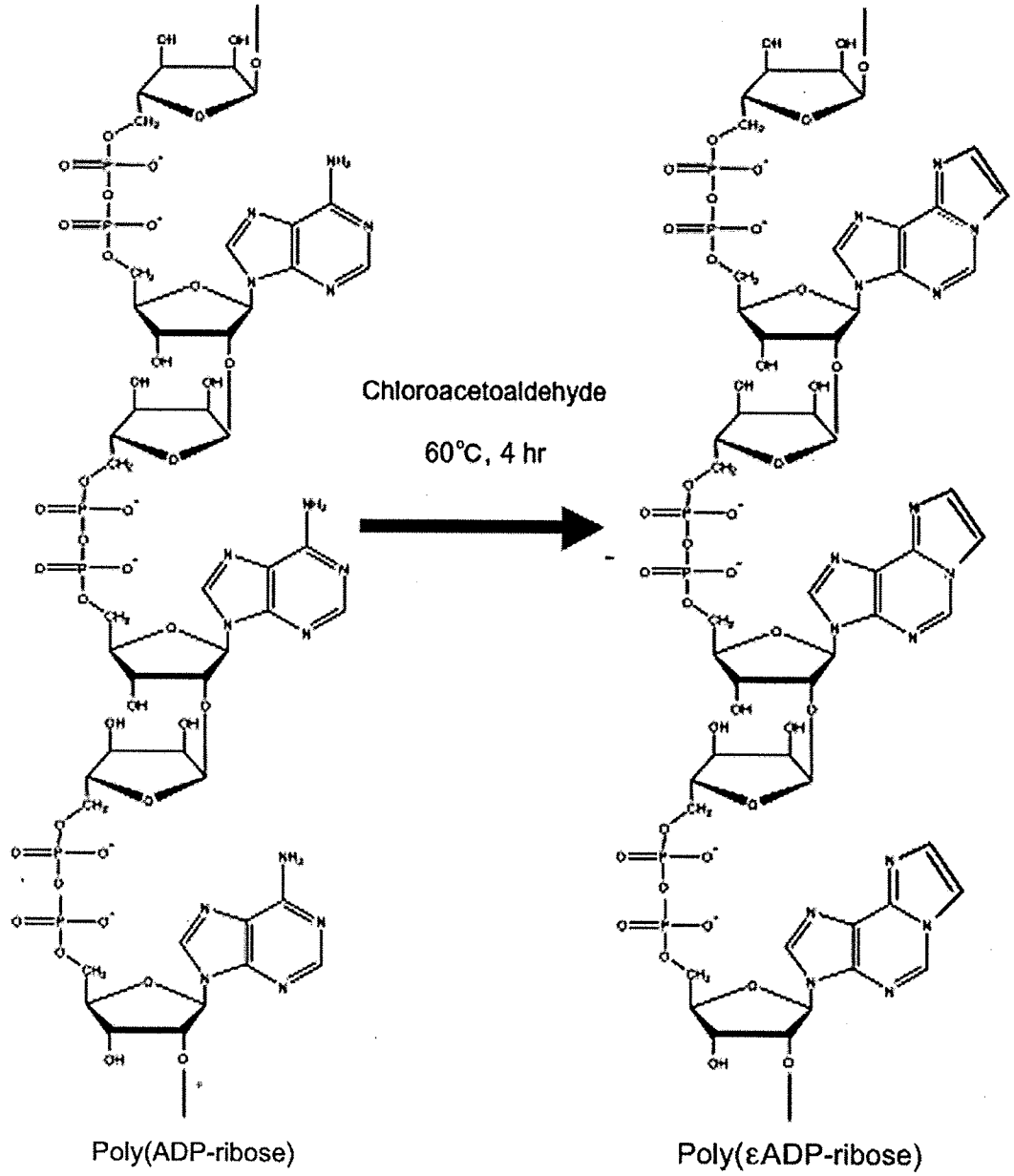

Fig. 1. Conversion of poly(ADP-ribose) to poly(εADP-ribose).

Invitrogen) and HeLa cells were lysed with a buffer containing 20 mM potassium phosphate (pH 7.5), 0.05% Triton X-100, 10 mM β-mercaptoethanol. Etheno NAD was purchased from Sigma.

Polyacrylamide gel electrophoresis (PAGE) and thin layer chromatography (TLC). PAGE (20%) of ^{32}P-poly(εADP-ribose) and ^{32}P-poly(ADP-ribose) was performed as described elsewhere [25]. TLC was carried out using polyethyleneimine-impregnented TLC plates (Macherey-Nagel) using a developing solvent consisting 3 M acetic acid, 0.1 M LiCl and 3 M Urea [21]. Radioactivity was measured using BAS2500 (Fuji Film).

High performance liquid chromatography (HPLC) and liquid chromatography mass spectrometry (LC–MS). HPLC (Shimadzu LC solution) was carried out using Develosil column (C30-UG-5, 046 × 250 mm, Nomura Chemicals). UV absorbance was monitored at 254 nm (Tosoh, UV-8000). Fluorescence was monitored (Shimadzu RF-10AXL) with excitation at 230 nm and emission at 410 nm. A linear gradient elution for 100 min using buffer A (0.1 M ammonium acetate) and buffer B (50 mM ammonium acetate – 50% acetonitrile) was performed, starting from 2% to 100% concentration of buffer B at a flow rate of 0.5 ml/min.

LC–MS was carried out by electrospray ionization method (Micromass ZQ, Waters). LC system (Series 1100, Agilent) was performed with Develosil C30-UG-5 column using buffer A and B as described above. A linear gradient starting from 2% to 50% concentration of buffer B was applied at a flow rate of 0.3 ml/min for 50 min. Two microgram of poly(εADP-ribose) were digested with 0.012 U of PDE at 25 °C overnight, treated with perchloric acid as described above, and soluble fraction was applied to HPLC. The collected fraction was then concentrated and prefiltrated (YM-3, Millipore) before LC–MS.

Preparation of 5″-phosphoribosyl etheno 5′-AMP (PR-εAMP) and etheno ADP-ribose (εADP-ribose). PR-AMP prepared from poly(ADP-ribose) [24] or ADP-ribose (Sigma) was mixed with the reaction mixture containing 0.1 M chloroacetaldehyde and 0.2 M ammonium acetate and reacted at 60 °C for 4 h. The reaction was stopped by adding ammonium solution to 0.8% (v/v) and applied to HPLC, and the fraction of PR-εAMP and εADP-ribose was collected. PR-εAMP and εADP-ribose (molecular mass of both compounds = 583) were further subjected to LC–MS.

Results and discussion

Etheno derivatization of poly(ADP-ribose) was carried out using the reaction condition for preparation of 1-N^6-etheno adenosine [23]. The UV spectrum of prepared poly(εADP-ribose) was similar to that of 1-N^6-etheno adenosine [26]. When poly(εADP-ribose) was digested with PDE and subjected to HPLC, a main peak of PR-εAMP (Fig. 2A) was observed and the amount of PR-AMP was only 1% of PR-εAMP (Fig. 2B). The conversion efficiency of adenine to εA residues in poly(ADP-ribose) was thus ≈99%. When the PR-εAMP fraction was subjected to LC–MS, molecular ion peaks at m/z = 584 (ES+) and 582 (ES-) were detected (Fig. 2C). These peaks matched to expected mass of PR-εAMP (molecular mass = 583) and the profile (Fig. 2C) was identical to that of standard PR-εAMP (data not shown).

^{32}P-poly(εADP-ribose) was subjected to 20% PAGE and TLC (Fig. 3A and B). A ladder pattern similar to ^{32}P-poly(ADP-ribose) was observed; however, the ladder of ^{32}P-poly(εADP-ribose) showed slightly slower mobility than that of ^{32}P-poly(ADP-ribose). After digestion with PDE, ^{32}P-poly(εADP-ribose) was almost completely digested to PR-εAMP and εAMP (Fig. 3A and B). In contrast, ^{32}P-poly(εADP-ribose) was not digested to εADP-ribose by GST-Parg whereas ^{32}P-poly(ADP-ribose)

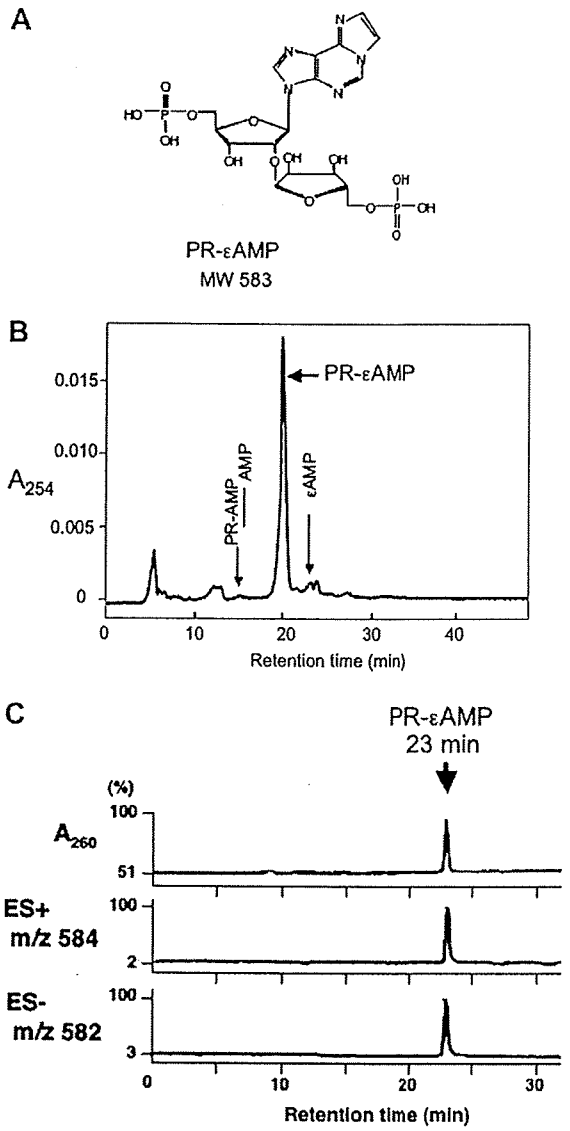

Fig. 2. HPLC and LC–MS of poly(εADP-ribose) after digestion with PDE. (A) Structure of PR-εAMP. (B) Poly(εADP-ribose) was digested with PDE and subjected to HPLC. Most of UV absorbance was eluted at the retention time of PR-εAMP. No peak was detected at the retention time for AMP. (C) The PR-εAMP fraction was subjected to LC–MS. Molecular ion peaks of m/z = 584 (ES+) and 582 (ES−) were detected at retention time of PR-εAMP.

was nearly completely digested to ADP-ribose and AMP. AMP is formed by Parg activity from protein-side terminal adenylate moiety, which is considered to be formed during preparation of poly(ADP-ribose) through detachment of poly(ADP-ribose) from protein by alkaline treatment [21]. When ^{32}P-poly(εADP-ribose) was incubated with increasing amount of GST-Parg at the extended time period (Fig. 3C), ^{32}P-poly(εADP-ribose) was again resistant to digestion by GST-Parg. Poly(εADP-ribose) was neither digested by Parg activity in the extract of HeLa cells nor Sf9 cells expressing rat Parg (Fig. 2D).

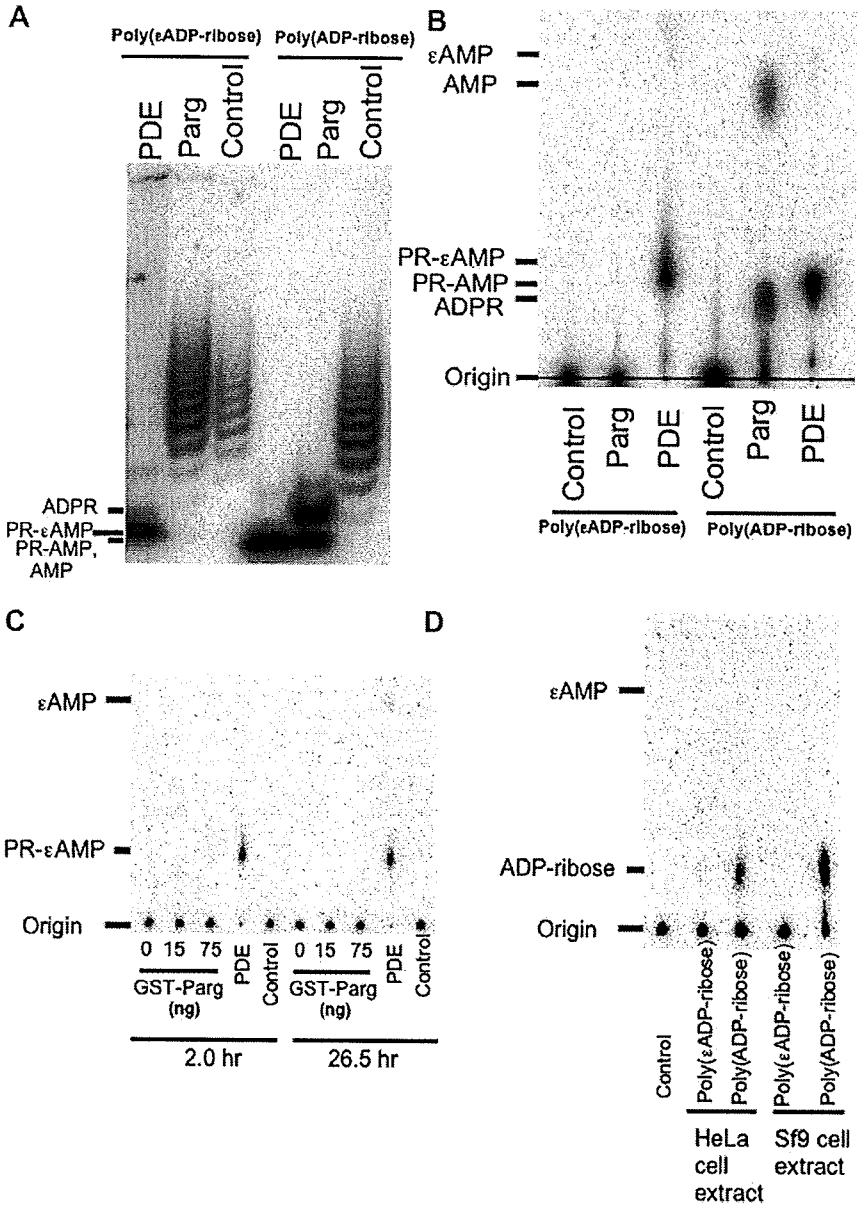

Fig. 3. Susceptibility of poly(εADP-ribose) to digestion by Parg and PDE. (A) PAGE (20%) of ^{32}P-poly(εADP-ribose) and ^{32}P-poly(ADP-ribose) after digestion with GST-Parg or PDE. Digestion of poly(ADP-ribose) by Parg to ADP-ribose (R_f value of 0.23) was observed, whereas digestion of ^{32}P-poly(εADP-ribose) by Parg to εADP-ribose (*Rf* value of 0.27) was not observed. (B) Analysis of the products in A by TLC. (C) ^{32}P-poly(εADP-ribose) and ^{32}P-poly(ADP-ribose) were subjected to TLC after digestion with GST-Parg or PDE. (D) ^{32}P-Poly(εADP-ribose) and ^{32}P-poly(ADP-ribose) were digested with the extracts of HeLa cells or Sf9 cells expressing rat Parg at 25 °C for 2 h.

We further tested whether poly(εADP-ribose) inhibits Parg activity using free poly(ADP-ribose) as substrate (Fig. 4). Increasing concentrations of poly(εADP-ribose) inhibited Parg activity. The IC_{50} value for poly(εADP-ribose) was approximately 3 μM (equivalent of εADP-ribose) in the presence of poly(ADP-ribose) at 2.6 μM (equivalent of ADP-ribose). In contrast, inhibition of GST-Parg activity by free εADP-ribose or etheno NAD was not observed (data not shown).

Oei et al. reported that poly(εADP-ribose) of their preparation could be degraded by Parg activity [20]. Their reaction was performed "at ambient temperature for 16 h" for synthesis of poly(εADP-ribose). Their reaction temperature was much lower compared to the temperature we applied, therefore, percentage of conversion to εA residues might be lower compared with our condition. Their polymer could contain modified εA residues only partially and could show much higher susceptibility to Parg activity compared with poly(εADP-ribose) which we prepared in this study.

Poly(εADP-ribose) may be useful to investigate function of Parg or the biological effects on cells after introduction

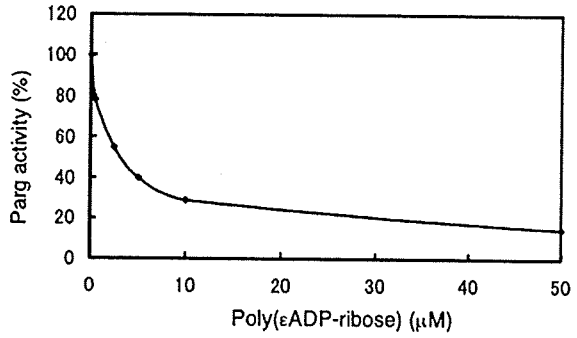

Fig. 4. Inhibition of Parg activity by poly(εADP-ribose). ^{32}P-Poly(ADP-ribose) at 2.6 μM (equivalent of ADP-ribose) was digested with GST-Parg in the presence of various concentration of poly(εADP-ribose) (equivalent of εADP-ribose) at 25 °C for 30 min.

into cells, because poly(εADP-ribose) might show extended half life within the cells compared with poly(ADP-ribose) due to high resistance to Parg activity.

This study also indicated that modification of adenine residues in poly(ADP-ribose) extensively decreases susceptibility to Parg activity. There are only a few effective PARG inhibitors [17,27–29]. Parg inhibitors may be developed by introducing modification on adenine residues of poly- or oligo(ADP-ribose).

Acknowledgments

We thank T. Sugimura and R. Dashwood for critical reading of the manuscript. This work was supported in part by a Grant-in-Aid for Cancer Research and Grant-in Aid for the Third Term Comprehensive 10-Year Strategy for Cancer Control from the Ministry of Health, Labour and Welfare of Japan, and a Grant-in-Aid from the Mitsubishi Foundation.

References

[1] V. Rolli, A. Ruf, A. Augustin, G.E. Schulz, J. Menissier-de Murcia, G. de Murcia, Poly(ADP-ribose) polymerase: structure and function, in: G. de Murcia, S. Shall (Eds.), From DNA damage and stress signaling to cell death. PolyADP-ribosylation reactions, Oxford University Press, New York, 2000, pp. 35–79.

[2] T. Sugimura, Poly(adenosine diphosphate ribose), Prog. Nucleic Acid Res. Mol. Biol. 13 (1973) 127–151.

[3] M. Masutani, H. Nakagama, T. Sugimura, Poly(ADP-ribosyl)ation in relation to cancer and autoimmune disease, Cell. Mol. Life Sci. 62 (2005) 769–783.

[4] V. Schreiber, F. Dantzer, J.C. Ame, G. de Murcia, Poly(ADP-ribose): novel functions for an old molecule, Nat. Rev. Mol. Cell Biol. 7 (2006) 517–528.

[5] M. Futai, D. Mizuno, T. Sugimura, Hydrolysis of the polymer formed from NAD with rat liver phosphodiesterase yielding nucleoside 5′ monophosphate, Biochem. Biophys. Res. Commun. 28 (1967) 395–399.

[6] M. Miwa, T. Sugimura, Splitting of the ribose-ribose linkage of poly(adenosine diphosphate-robose) by a calf thymus extract, J. Biol. Chem. 246 (1971) 6362–6364.

[7] W. Lin, J.C. Ame, N. Aboul-Ela, E.L. Jacobson, M.K. Jacobson, Isolation and characterization of the cDNA encoding bovine poly(ADP-ribose) glycohydrolase, J. Biol. Chem. 272 (1997) 11895–11901.

[8] U. Cortes, W.M. Tong, D.L. Coyle, M.L. Meyer-Ficca, R.G. Meyer, V. Petrilli, Z. Herceg, E.L. Jacobson, M.K. Jacobson, Z.Q. Wang, Depletion of the 110-kilodalton isoform of poly(ADP-ribose) glycohydrolase increases sensitivity to genotoxic and endotoxic stress in mice, Mol. Cell Biol. 24 (2004) 7163–7178.

[9] D.W. Koh, A.M. Lawler, M.F. Poitras, M. Sasaki, S. Wattler, M.C. Nehls, T. Stoger, G.G. Poirier, V.L. Dawson, T.M. Dawson, Failure to degrade poly(ADP-ribose) causes increased sensitivity to cytotoxicity and early embryonic lethality, Proc. Natl. Acad. Sci. USA 101 (2004) 17699–17704.

[10] M. Masutani, A. Gunji, H. Ogino, A. Uemura, A. Shibata, N. Kamada, K. Jishage, H. Nakagama, T. Sugimura, Functional analysis of poly(ADP-ribose) glycohydrolase: Hypersensitivity to DNA damaging agents and spontaneous development of renal lesions under Parg-deficiency, Med. Sci. 11 (Suppl. 1) (2005) 22.

[11] W. Ying, M.B. Sevigny, Y. Chen, R.A. Swanson, Poly(ADP-ribose) glycohydrolase mediates oxidative and excitotoxic neuronal death, Proc. Natl. Acad. Sci. USA 98 (2001) 12227–12232.

[12] A. Tulin, N.M. Naumova, A.K. Menon, A.C. Spradling, Drosophila poly(ADP-Ribose) glycohydrolase mediates chromatin structure and SIR2-dependent silencing, Genetics 172 (2006) 363–371.

[13] M.Y. Kim, S. Mauro, N. Gevry, J.T. Lis, W.L. Kraus, NAD+dependent modulation of chromatin structure and transcription by nucleosome binding properties of PARP-1, Cell 119 (2004) 803–814.

[14] P. Chang, M.K. Jacobson, T.J. Mitchison, Poly(ADP-ribose) is required for spindle assembly and structure, Nature 432 (2004) 645–649.

[15] S.A. Andrabi, N.S. Kim, S.W. Yu, H. Wang, D.W. Koh, M. Sasaki, J.A. Klaus, T. Otsuka, Z. Zhang, R.C. Koehler, P.D. Hurn, G.G. Poirier, V.L. Dawson, T.M. Dawson, Poly(ADP-ribose) (PAR) polymer is a death signal, Proc. Natl. Acad. Sci. USA 103 (2006) 18308–18313.

[16] S.W. Yu, S.A. Andrabi, H. Wang, N.S. Kim, G.G. Poirier, T.M. Dawson, V.L. Dawson, Apoptosis-inducing factor mediates poly(ADP-ribose) (PAR) polymer-induced cell death, Proc. Natl. Acad. Sci. USA 103 (2006) 18314–18319.

[17] L. Tentori, C. Leonetti, M. Scarsella, A. Muzi, M. Vergati, O. Forini, P.M. Lacal, F. Ruffini, B. Gold, W. Li, J. Zhang, G. Graziani, Poly(ADP-ribose) glycohydrolase inhibitor as chemosensitiser of malignant melanoma for temozolomide, Eur. J. Cancer 41 (2005) 2948–2957.

[18] J.F. Haince, M.E. Ouellet, D. McDonald, M.J. Hendzel, G.G. Poirier, Dynamic relocation of poly(ADP-ribose) glycohydrolase isoforms during radiation-induced DNA damage, Biochim. Biophys. Acta 1763 (2006) 226–237.

[19] J.P. Gagne, M.J. Hendzel, A. Droit, G.G. Poirier, The expanding role of poly(ADP-ribose) metabolism: current challenges and new perspectives, Curr. Opin. Cell Biol. 18 (2006) 145–151.

[20] S.L. Oei, J. Griesenbeck, G. Buchlow, D. Jorcke, P. Mayer-Kuckuk, T. Wons, M. Ziegler, NAD+ analogs substituted in the purine base as substrates for poly(ADP-ribosyl) transferase, FEBS Lett. 397 (1996) 17–21.

[21] T. Shimokawa, M. Masutani, S. Nagasawa, T. Nozaki, N. Ikota, Y. Aoki, H. Nakagama, T. Sugimura, Isolation and cloning of rat poly(ADP-ribose) glycohydrolase: presence of a potential nuclear export signal conserved in mammalian orthologs, J. Biochem. (Tokyo) 126 (1999) 748–755.

[22] R. Alvarez-Gonzalez, M.K. Jacobson, Characterization of polymers of adenosine diphosphate ribose generated in vitro and in vivo, Biochemistry 26 (1987) 3218–3224.

[23] M.K. Jacobson, D.M. Payne, R. Alvarez-Gonzalez, H. Juarez-Salinas, J.L. Sims, E.L. Jacobson, Determination of in vivo levels of polymeric and monomeric ADP-ribose by fluorescence methods, Meth. Enzymol. 106 (1984) 483–494.

[24] M. Ikejima, G. Marsischky, D.M. Gill, Direction of elongation of poly(ADP-ribose) chains. Addition of residues at the polymerase-proximal terminus, J. Biol. Chem. 262 (1987) 17641–17650.
[25] P.L. Panzeter, F.R. Althaus, High resolution size analysis of ADP-ribose polymers using modified DNA sequencing gels, Nucleic Acids Res. 18 (1990) 2194.
[26] J.A. Secrist 3rd, J.R. Barrio, N.J. Leonard, G. Weber, Fluorescent modification of adenosine-containing coenzymes. Biological activities and spectroscopic properties, Biochemistry 11 (1972) 3499–3506.
[27] J.T. Slama, N. Aboul-Ela, D.M. Goli, B.V. Cheesman, A.M. Simmons, M.K. Jacobson, Specific inhibition of poly(ADP-ribose) glycohydrolase by adenosine diphosphate (hydroxymethyl)pyrrolidinediol, J. Med. Chem. 38 (1995) 389–393.
[28] M. Masutani, T. Shimokawa, M. Igarashi, M. Hamada, A. Shibata, S. Oami, T. Nozaki, H. Nakagama, T. Sugimura, T. Takeuchi, M. Hori, Inhibition of poly(ADP-ribose) glycohydrolase activity by cyclic peptide antibiotics containing piperazic acid residues, Proc. Japan Acad. Ser. B 78 (2002) 15–17.
[29] K. Aoki, H. Maruta, F. Uchiumi, T. Hatano, T. Yoshida, S. Tanuma, A macrocircular ellagitannin, oenothein B, suppresses mouse mammary tumor gene expression via inhibition of poly(ADP-ribose) glycohydrolase, Biochem. Biophys. Res. Commun. 210 (1995) 329–337.

BMC Genomics

BioMed Central

Research article

Open Access

Loss of *Parp-1* affects gene expression profile in a genome-wide manner in ES cells and liver cells

Hideki Ogino[1,2], Tadashige Nozaki[2], Akemi Gunji[2], Miho Maeda[3], Hiroshi Suzuki[4], Tsutomu Ohta[5], Yasufumi Murakami[3], Hitoshi Nakagama[2], Takashi Sugimura[2] and Mitsuko Masutani*[1,2]

Address: [1]ADP-ribosylation in Oncology Project, National Cancer Center Research Institute, 1-1, Tsukiji 5-chome, Chuo-ku, Tokyo 104-0045, Japan, [2]Biochemistry Division, National Cancer Center Research Institute, 1-1, Tsukiji 5-chome, Chuo-ku, Tokyo 104-0045, Japan, [3]Department of Biological Science & Technology, Faculty of Industrial Science & Technology, Tokyo University of Science, 2641, Yamazaki, Noda, Chiba 278-8510, Japan, [4]Chugai Pharmaceutical Co Ltd., 1-135, Komakado, Gotemba, Shizuoka, 412-0038, Japan and [5]Center for Medical Genomics, National Cancer Center Research Institute, 1-1, Tsukiji 5-chome, Chuo-ku, Tokyo 104-0045, Japan

Email: Hideki Ogino - hogino@gan2.res.ncc.go.jp; Tadashige Nozaki - nozaki@cc.osaka-dent.ac.jp; Akemi Gunji - agunji@ntmc.hosp.go.jp; Miho Maeda - mihmaeda@gan2.res.ncc.go.jp; Hiroshi Suzuki - hisuzuki@obihiro.ac.jp; Tsutomu Ohta - cota@gan2.res.ncc.go.jp; Yasufumi Murakami - yasufumi@rs.noda.tus.ac.jp; Hitoshi Nakagama - hnakagam@gan2.res.ncc.go.jp; Takashi Sugimura - tsugimur@gan2.res.ncc.go.jp; Mitsuko Masutani* - mmasutan@gan2.res.ncc.go.jp

* Corresponding author

Published: 7 February 2007

BMC Genomics 2007, 8:41 doi:10.1186/1471-2164-8-41

Received: 5 August 2006

Accepted: 7 February 2007

This article is available from: http://www.biomedcentral.com/1471-2164/8/41

Abstract

Background: Many lines of evidence suggest that poly(ADP-ribose) polymerase-1 (Parp-1) is involved in transcriptional regulation of various genes as a coactivator or a corepressor by modulating chromatin structure. However, the impact of *Parp-1*-deficiency on the regulation of genome-wide gene expression has not been fully studied yet.

Results: We employed a microarray analysis covering 12,488 genes and ESTs using mouse *Parp-1*-deficient (*Parp-1*$^{-/-}$) embryonic stem (ES) cell lines and the livers of *Parp-1*$^{-/-}$ mice and their wild-type (*Parp-1*$^{+/+}$) counterparts. Here, we demonstrate that of the 9,907 genes analyzed, in *Parp-1*$^{-/-}$ ES cells, 9.6% showed altered gene expression. Of these, 6.3% and 3.3% of the genes were down- or up-regulated by 2-fold or greater, respectively, compared with *Parp-1*$^{+/+}$ ES cells ($p < 0.05$). In the livers of *Parp-1*$^{-/-}$ mice, of the 12,353 genes that were analyzed, 2.0% or 1.3% were down- and up-regulated, respectively ($p < 0.05$). Notably, the number of down-regulated genes was higher in both ES cells and livers, than that of the up-regulated genes. The genes that showed altered expression in ES cells or in the livers are ascribed to various cellular processes, including metabolism, signal transduction, cell cycle control and transcription. We also observed expression of the genes involved in the pathway of extraembryonic tissue development is augmented in *Parp-1*$^{-/-}$ ES cells, including *H19*. After withdrawal of leukemia inhibitory factor, expression of *H19* as well as other trophoblast marker genes were further up-regulated in *Parp-1*$^{-/-}$ ES cells compared to *Parp-1*$^{+/+}$ ES cells.

Conclusion: These results suggest that *Parp-1* is required to maintain transcriptional regulation of a wide variety of genes on a genome-wide scale. The gene expression profiles in *Parp-1*-deficient cells may be useful to delineate the functional role of Parp-1 in epigenetic regulation of the genomes involved in various biological phenomena.